

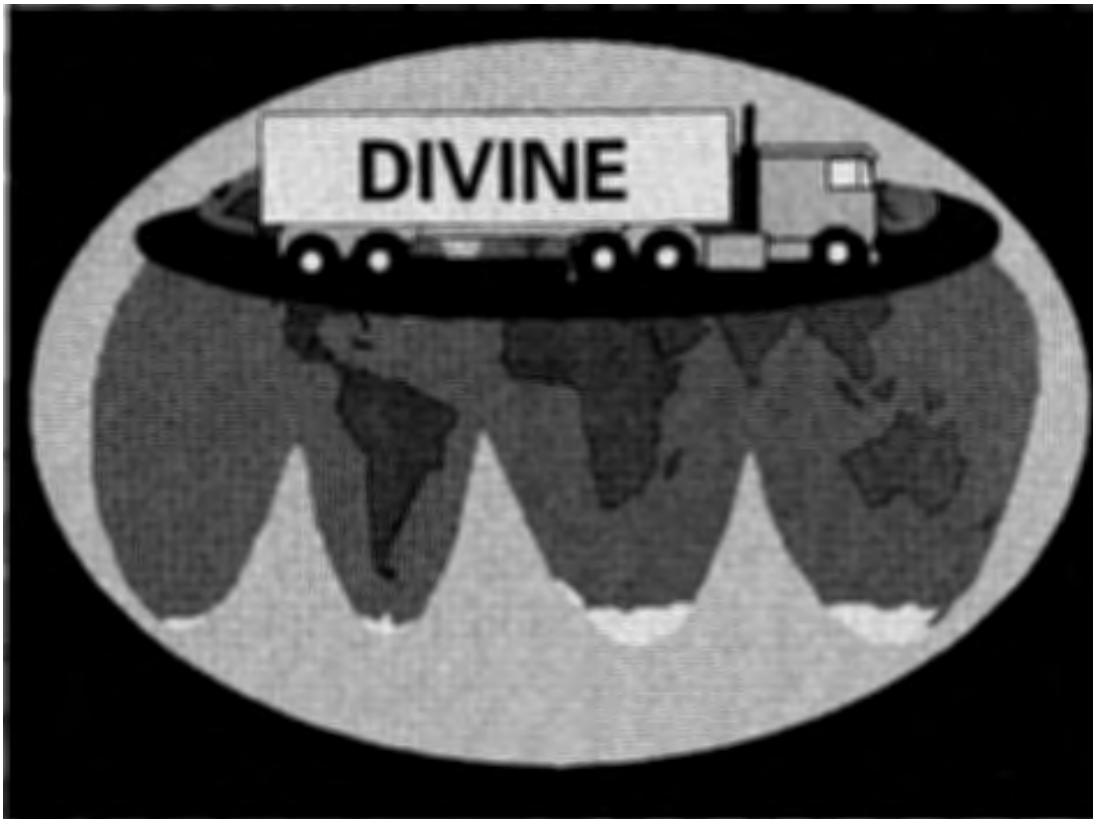
Analysis of Pavement Structural Variability



PB97-171961

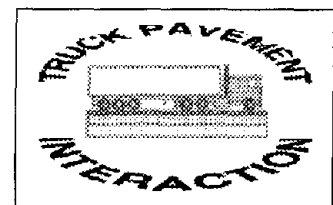
PUBLICATION NO. FHWA-RD-97-072

JUNE 1997



U.S. Department of Transportation
Federal Highway Administration

Research and Development
Turner-Fairbank Highway Research Center
6300 Georgetown Pike
McLean, VA 22101-2296



REPRODUCED BY: **NTIS**
U.S. Department of Commerce
National Technical Information Service
Springfield, Virginia 22161

FOREWORD

This report is one of the final reports submitted to the Organisation for Economic Co-operation and Development (OECD) Dynamic Interaction Vehicle-INfrastructure Experiment (DIVINE) project committee by the Federal Highway Administration, Office of Engineering Research and Development. An analysis was performed on the data collected from the accelerated loading test conducted under the DIVINE project. This report focuses on determining the extent to which initial pavement variability due to construction practices and differences in material quality has an effect on overall pavement performance, especially as it is compared to the effects under the actions of applied dynamic loading on pavement performance.

The findings in this report provide useful information on the effect of pavement structural variability and vehicle dynamic wheel force on pavement performance.




Charles J. Nemmers, Director
Office of Engineering and
Highway Operations
Research and Development

NOTICE

This document is disseminated under the sponsorship of the Department of Transportation in the interest of information exchange. The United States Government assumes no liability for its contents or use thereof. This report does not constitute a standard, specification, or regulation.

The United States Government does not endorse products or manufactures. Trade and manufactures' names appear in this report only because they are considered essential to the object of the document.

Technical Report Documentation Page

1. Report No. FHWA-RD-97-072		2.  PB97-171961		3. Recipient's Catalog No.	
4. Title and Subtitle ANALYSIS OF PAVEMENT STRUCTURAL VARIABILITY				5. Report Date June 1997	
				6. Performing Organization Code HNR-30	
7. Author(s) William J. Kenis and Weijun Wang				8. Performing Organization Report No.	
9. Performing Organization Name and Address Pavement Performance Division, HNR-30 Turner-Fairbank Highway Research Center 6300 Georgetown Pike McLean, Virginia 22101-2296				10. Work Unit No. (TRAIS) 3C4A	
				11. Contract or Grant No.	
12. Sponsoring Agency Name and Address Office of Engineering Research and Development Federal Highway Administration 6300 Georgetown Pike McLean, Virginia 22101-2296				13. Type of Report and Period Covered Final Report October 1994 - March, 1997	
				14. Sponsoring Agency Code	
15. Supplementary Notes FHWA contact: William Kenis, HNR - 30 The entire DIVINE team, especially J. de Pont, B. Pidwerbesky, B. Steven, K. Sharp, R. Addis, P. Sweatman and FHWA in-house staff team members B. Brademeyer, J. Hammouda and D. George are acknowledged for their contribution to this research.					
16. Abstract It is well known that during construction of any highway pavement, variations in layer material quality, environmental influences, homogeneity, and variations in construction technique all lead to nonuniform spatial variations in the layer material properties / layer thicknesses comprising the pavement structure. As vehicle loads are applied to the pavement, the spatial variations result in the development of nonuniform spatial distributions of stress, strain, and deformation within the pavement, in turn causing nonuniform distributions of defects in the pavement. (External influences arising after construction such as the infiltration of water, drying out and freeze thaw cycles will also contribute to such nonuniform spatial distribution of defects). The nonuniform distribution of defects eventually manifest into visible differences in pavement distress, e.g. variations in area cracked, and variations in permanent deformation along the wheel track called rutting. It is an important aspect of the Dynamic Interaction Vehicle - Infrastructure Experiment (DIVINE) program to attempt to distinguish between the development of pavement distress resulting from initial variations in materials properties / layer thicknesses and from variations in the dynamic wheel forces imposed to the pavement due to tire-suspension dynamics. The analyses presented in this report were conducted to determine if such differences in the level of these two phenomena is detectable. In the analyses initial structural variability of the Canterbury Accelerated Pavement Testing Indoor Facility at University of Canterbury, New Zealand (CAPTIF) pavement is investigated in terms of two known measured variables, thickness and falling weight deflectometer (FWD) center deflection. The study revealed that pavement structural variability indeed influences pavement performance, such as pavement rutting and cracking; the pavement structural variability must be taken into consideration when investigating the effect of heavy vehicle induced dynamic load on pavement performance. The study also showed that steel suspension usually generates higher dynamic wheel force and causes more pavement damage than air suspension; and exponential relationships exist between pavement performance, wheel force and pavement initial condition.					
17. Key Words Pavement performance, structural variability, cross correlation analysis, OECD DIVINE project			18. Distribution Statement No restriction. This document is available to the public through the National Technical Information Service, Springfield, Virginia 22161		
19. Security Classif. (of this report) Unclassified		20. Security Classif. (of this page) Unclassified		21. No. of Pages 49	22. Price

SI* (MODERN METRIC) CONVERSION FACTORS

APPROXIMATE CONVERSIONS TO SI UNITS

Symbol	When You Know	Multiply By	To Find	Symbol
LENGTH				
in	inches	25.4	millimeters	mm
ft	feet	0.305	meters	m
yd	yards	0.914	meters	m
mi	miles	1.61	kilometers	km
AREA				
in ²	square inches	645.2	square millimeters	mm ²
ft ²	square feet	0.093	square meters	m ²
yd ²	square yards	0.836	square meters	m ²
ac	acres	0.405	hectares	ha
mi ²	square miles	2.59	square kilometers	km ²
VOLUME				
fl oz	fluid ounces	29.57	milliliters	mL
gal	gallons	3.785	liters	L
ft ³	cubic feet	0.028	cubic meters	m ³
yd ³	cubic yards	0.765	cubic meters	m ³
MASS				
oz	ounces	28.35	grams	g
lb	pounds	0.454	kilograms	kg
T	short tons (2000 lb)	0.907	megagrams (or "metric ton")	Mg (or "t")
TEMPERATURE (exact)				
°F	Fahrenheit temperature	5(F-32)/9 or (F-32)/1.8	Celsius temperature	°C
ILLUMINATION				
fc	foot-candles	10.76	lux	lx
fl	foot-Lamberts	3.426	candela/m ²	cd/m ²
FORCE and PRESSURE or STRESS				
lbf	poundforce	4.45	newtons	N
lbf/in ²	poundforce per square inch	6.89	kilopascals	kPa

APPROXIMATE CONVERSIONS FROM SI UNITS

Symbol	When You Know	Multiply By	To Find	Symbol
LENGTH				
mm	millimeters	0.039	inches	in
m	meters	3.28	feet	ft
m	meters	1.09	yards	yd
km	kilometers	0.621	miles	mi
AREA				
mm ²	square millimeters	0.0016	square inches	in ²
m ²	square meters	10.764	square feet	ft ²
m ²	square meters	1.195	square yards	yd ²
ha	hectares	2.47	acres	ac
km ²	square kilometers	0.386	square miles	mi ²
VOLUME				
mL	milliliters	0.034	fluid ounces	fl oz
L	liters	0.264	gallons	gal
m ³	cubic meters	35.71	cubic feet	ft ³
m ³	cubic meters	1.307	cubic yards	yd ³
MASS				
g	grams	0.035	ounces	oz
kg	kilograms	2.202	pounds	lb
Mg (or "t")	megagrams (or "metric ton")	1.103	short tons (2000 lb)	T
TEMPERATURE (exact)				
°C	Celsius temperature	1.8C + 32	Fahrenheit temperature	°F
ILLUMINATION				
lx	lux	0.0929	foot-candles	fc
cd/m ²	candela/m ²	0.2919	foot-Lamberts	fl
FORCE and PRESSURE or STRESS				
N	newtons	0.225	poundforce	lbf
kPa	kilopascals	0.145	poundforce per square inch	lbf/in ²

* SI is the symbol for the International System of Units. Appropriate rounding should be made to comply with Section 4 of ASTM E380.

TABLE OF CONTENTS

<u>Section</u>	<u>Page</u>
OBJECTIVE	1
INTRODUCTION	1
SUMMARY OF CAPTIF PAVEMENT CONSTRUCTION	1
ASSUMPTIONS AND EQUATIONS	2
ANALYSES	5
Variations Defining Initial Conditions	6
Spatial Variation of Layer Thickness at Construction	6
Spatial Variation of FWD Layer Deflections at Construction	6
Spatial Variation of Layer Moduli at Construction	7
Spatial Variation of Initial Equivalent Stiffness at Construction	7
Spatial Variation of FWD Deflections at Beginning of Test (after preloading)	7
Correlation between FWD Surface Deflections at Beginning of Test	8
Variations of Selected Variables at Different Load Repetitions	8
Dynamic Load Coefficient (DLC) and International Roughness Index (IRI)	8
Profiles	9
Vertical Surface Deformation (VSD)	10
Rut Depth	10
Cross Correlation	11
Linear Cross Correlations between Initial Variability and Performance Measures	11
Linear Cross Correlations between Wheel Force and Other Variables	12
Linear Cross Correlation between Cracking and Rut Depth	13
Linear Cross Correlation between Final (1700-k) Profile and Profiles at other Load Repetitions	13
Pseudo Nonlinear Cross Correlations between VSD and Other Variables	13
Pseudo Nonlinear Cross Correlation between Wheel Force and other Variables	14
Pseudo Nonlinear Cross Correlation between Performance Measures and other Variables	14
CONCLUSIONS	15
REFERENCE	43

LIST OF FIGURES

<u>Figure</u>	<u>Page</u>
1. Layer Thickness, Inner Track	24
2. Layer Thickness, Outer Track	24
3. Unit Load Layer Deflection at Construction, Inner Track	25
4. Unit Load Layer Deflection at Construction, Outer Track	25
5. Layer Moduli, Inner Track (Initial)	26
6. Layer Moduli, Outer Track (Initial)	26
7. Equivalent Pavement Stiffness	26
8a. Pavement FWD Surface Deflection at 20 k	27
8b. Pavement FWD Surface Deflection, at Construction and at 20 k, Inner Track	27
8c. Pavement FWD Surface Deflection, at Construction and at 20 k, Outer Track	27
9. DLC and IRI vs. Load Repetitions	28
10a. Inner Track Profile at Different Load Repetitions	28
10b. Outer Track Profile at Different Load Repetitions	28
11a. Inner Track Profiles	29
11b. Outer Track Profiles	29
11c. Change of Profile from Beginning to End of Test	29
12a. Inner Track VSD	30
12b. Outer Track VSD	30
12c. Change of VSD from Beginning to End of Test	30
12d. Mean VSD Change Rate, All Data	31
12e. Correlation Coefficient between Inner and Outer Track VSD	31
13a. Mean Rut Depth vs. Load Repetitions	32
13b. Comparison of Rut Depth Variations of Outer and Inner Tracks, Select Data	32
14a. Inner Track Rut Depth at Beginning and End of Test	33
14b. Outer Track Rut Depth at Beginning and End of Test	33
14c. Change of Rut Depth at Beginning and End of Test	33
14d. Mean Surface Rut Depth Change Rate, All Data	34
14e. Correlation Coefficient between Inner and Outer Track Rut Depth	34
15. Cross Correlation between FWD Surface Deflection at 20 k and VSD (Inner - All Data, Outer - Select Data)	35
16. Cross Correlation between FWD Surface Deflection at 20 k and Rut Depth (Inner - All Data, Outer - Select Data)	35

LIST OF FIGURES
(Continued)

<u>Figure</u>	<u>Page</u>
17a. Correlation between FWD Surface Deflection at 20 k and Total Linear Cracking (All Data)	36
17b. Correlation between FWD Surface Deflection at 20 k and Longitudinal Linear Cracking (All Data)	36
17c. Correlation between FWD Surface Deflection at 20 k and Transverse Linear Cracking (All Data)	36
18. Cross Correlation between Wheel Force and FWD Surface Deflection at 20 k (Inner - All Data, Outer - Select Data)	37
19. Cross Correlation between Wheel Force and VSD (Inner - All Data, Outer - Select Data)	37
20a. Cross Correlation between Wheel Force and Total Cracking (All Data)	38
20b. Cross Correlation between Wheel Force and Longitudinal Cracking	38
20c. Cross Correlation between Wheel Force and Transverse Cracking (All Data)	38
21a. Cross Correlation between Rut Depth and Linear Cracking Inner Track, All Data	39
21b. Cross Correlation between Rut Depth and Linear Cracking Outer Track, All Data	39
22. Correlation between Profile at 1700 k and Profiles at Other Load Repetitions (All Data)	40
23. Cross Correlation between VSD and (Wheel Force*FWD) (Inner - All Data, Outer - Select Data)	40
24. Cross Correlation between VSD and (Wheel Force/FWD) (Inner - All Data, Outer - Select Data)	40
25a. Correlation between Wheel Force and (VSD ⁿ /FWD), Inner Track (All Data)	41
25b. Correlation between Wheel Force and (VSD ⁿ /FWD), Outer Track (Select Data)	41
25c. Correlation between Wheel Force and (VSD ^{1/3} /FWD) (Inner - All Data, Outer - Select Data)	41
26a. Cross Correlation between Wheel Force and (VSD/FWD ³), All Data	42
26b. Cross Correlation between Wheel Force and (VSD/FWD ³), Select Data	42

LIST OF TABLES

<u>Table</u>	<u>Page</u>
1. Statistics of CAPTIF Pavement Layer Thickness	18
2. Statistics of CAPTIF Pavement Unit Layer Deflection at Construction (FWD Data)	18
3. Statistics of CAPTIF Pavement Unit Surface Deflection at Beginning of Test (at 20 k, FWD Data)	18
4. Statistics of CAPTIF Pavement Layer Modulus	19
5. Statistics of CAPTIF Pavement Equivalent Stiffness	19
6. Statistics of Pavement Elevation (Profile, m)	20
7. Statistics of Pavement Vertical Surface Deformation (VSD, mm)	21
8. Statistics of Pavement Rut Depth (mm)	22
9. Correlation between Assumed CAPTIF Test Pavement Performance Models and Measured Data	23

ANALYSIS OF PAVEMENT STRUCTURAL VARIABILITY

OBJECTIVE

The objective of this research is to determine the extent to which “initial” pavement variability due to construction practices and differences in material quality has an effect on overall pavement performance, especially as it is compared to the effects under the actions of applied dynamic loading on pavement performance.

INTRODUCTION

It is well known that during construction of any highway pavement, variations in layer material quality, environmental influences, homogeneity, and variations in construction technique all lead to nonuniform spatial variations in the layer material properties/layer thicknesses comprising the pavement structure. As vehicle loads are applied to the pavement, the spatial variations result in the development of nonuniform spatial distributions of stress, strain, and deformation within the pavement, in turn causing nonuniform distributions of defects in the pavement (external influences arising after construction such as the infiltration of water, drying out and freeze thaw cycles will also contribute to such nonuniform spatial distribution of defects). The nonuniform distribution of defects eventually manifest into visible differences in pavement distress, e.g. variations in area cracked, and variations in permanent deformation along the wheel track called rutting. It is an important aspect of the DIVINE program to attempt to distinguish between the development of pavement distress resulting from initial variations in materials properties/layer thicknesses and from variations in the dynamic wheel forces imposed to the pavement due to tire-suspension dynamics.

The analysis presented herein is conducted to determine if such differences in the level of these two phenomena is detectable. In the analysis initial structural variability of the Canterbury Accelerated Pavement Testing Indoor Facility at University of Canterbury, New Zealand (CAPTIF) pavement is investigated in terms of two known measured variables, thickness and falling weight deflectometer (FWD) center deflection. FWD deflections were selected to represent the combined effect of material variability existing in the subgrade, base, and AC surface for both the inner and outer tracks.

SUMMARY OF CAPTIF PAVEMENT CONSTRUCTION

The detailed structural and geometrical make-up of the CAPTIF test pavement and descriptions of the conduct of testing are presented elsewhere, however to facilitate continuity of thought, the main points are summarized.⁽¹⁾ The test pavement consists of three layers, 88 mm of asphalt concrete, and 200 mm granular base over a 1200 mm silty clay subgrade layer. It is contained in a circular concrete trough 58 m in centerline circumference, 4-m wide and 1.5 m deep. The 4-m wide circular test pavement accommodates an inner and an outer track so as to carry two

different axle suspensions: a single wheeled air suspension traveling over the inner track and a single wheeled steel suspension traveling over the outer track. Each wheel accommodates a single wide-base tire and was statically loaded to 49 kN during trafficking. During construction different types of in-situ nondestructive tests (NDT) were performed on each pavement layer in each wheel track: moisture content, density, thickness, California Bearing Ratio (CBR, subgrade only), FWD deflection basin data on each pavement layer, Loadman tests (base course only) and dynamic cone penetrometer tests. For this analysis layer thickness and FWD centerline deflection at each 1 m of the 58 stations around the test track, on the top of the subgrade, base and AC surface, for both the inner and outer wheel paths were used to represent the total variability of the pavement. At each station three drops at a given load level were made. The following summarizes the initial FWD deflection data used in this analysis:

Subgrade: 25 and 40 kN (**used centerline, third drop at 40 kN**)
 Base: 16.5 and 25 kN (**used centerline, third drop at 25 kN**)
 Asphalt: 20, 40, and 60 kN (**used centerline, third drop at 60 kN**)

The radius of the FWD load plate is 150 mm. The actual layer thicknesses measured at 1-m intervals (same locations as FWD drops) in each wheel path around the test loop were used.

ASSUMPTIONS AND EQUATIONS

The following assumptions were used to estimate layer moduli:

1. A three layer system of AC, base, and subgrade with Poisson's ratio taken as 0.4 for all layers.
2. FWD deflection directly under the center of the load applied to each of the three layers is the best estimator of the over all structural integrity of the over all system, the base-subgrade system and the subgrade by itself.
3. In order to assess the material variability of the layers, the concepts of Odemark and Boussinesq were used to calculate the individual layer modulus at 1-m intervals around the track. The principle of Odemark, also known as the “method of equivalent thickness,” is normally used to transform a system of n layers of different layer moduli to a single layer of equivalent stiffness where all layers have the same modulus. In this study we used these hypotheses to calculate the individual layer modulus and to transform the top two layers of the given three layer system to a single layer of equivalent stiffness.

For a uniform half space, Boussinesq's equation for deflection $D(z)$ under the center of loading at any depth z is

$$D(z) = 2(1 - \nu^2) \frac{qa}{E} \left[F_b \right] \quad (1)$$

where q is the applied pressure, a the radius of the loading area, E the modulus of the half space, μ is Poisson's ratio and F_b the Boussinesq single layer deflection factor expressed by the closed form solution⁽²⁾:

$$F_b = \left[\sqrt{1 + \left(\frac{z}{a}\right)^2} - \frac{z}{a} \right] \left[1 + \left(\left(\frac{z}{a}\right) \div \left(2(1-\nu) \sqrt{1 + \left(\frac{z}{a}\right)^2} \right) \right) \right] \quad (2)$$

where z is the depth into the uniform Boussinesq solid. For deflection under the center of loading at the top of the subgrade $D_{0,3}$, $F_b = 1$, and equation (1) reduces to:

$$D_{0,3} = 2(1-\nu^2) \frac{qa}{E_3} \quad (3)$$

Equation (3) was used to obtain the subgrade modulus E_3 from FWD deflections on the top of the subgrade and at 1-m intervals around each wheel path of the test loop.

For a two layer system of base and subgrade the deflection $D_{0,2}$ directly under the center of the load plate on the top of the base course may be approximated by:

$$D_{0,2} = 2(1-\nu^2) \frac{qa}{E_3 E_2} [E_3 + F_b(E_2 - E_3)] \quad (4)$$

where

$$F_b = \left[\sqrt{1 + \left(\frac{h_e}{a}\right)^2} - \left(\frac{h_e}{a}\right) \right] \left[1 + \left(\left(\frac{h_e}{a}\right) \div \left(2(1-\nu_2) \sqrt{1 + \left(\frac{h_e}{a}\right)^2} \right) \right) \right] \quad (5)$$

$$h_e = h_2 \left(\frac{E_2}{E_3} \right)^{1/3} \quad (6)$$

is the thickness of subgrade material needed to replace the current thickness of base in order to

maintain stiffness equivalent to that of the base; E_2 and E_3 are modulus of base and subgrade, respectively. Equations (4), (5), and (6) were used in an iterative process to determine the modulus of the base course E_2 based on FWD deflections on the top of the base course with assuming that the modulus of the subgrade is known. The base course modulus was also calculated at 1-m intervals around the track.

Equations (4) through (6) were also used to determine the modulus of the AC layer by using the same procedure as that used for determining base course modulus. In this case though, h_e in equation (6) is now given as:

$$h_e = \left[h_1 + h_2 \left(\frac{E_2}{E_1} \right)^{1/3} \right] \left[\left(\frac{E_1}{E_3} \right)^{1/3} \right] \quad (7)$$

where the subscripts 2 and 3 in equation (6) are replaced by the subscripts 1 and 3 respectively, and E_1 is AC layer modulus. Note that in this case both base and AC layers are transformed to an equivalent thickness of subgrade. It is further assumed that the moduli of the base and subgrade are known.

Knowing the modulus and thickness of the base and AC layers at every station (1-m intervals around the track), equations (8) and (9) were used to calculate “equivalent” AC stiffness, S_{AC} , of these two layers:

$$S_{AC} = E_1 \frac{h_e^3}{12(1-\nu^2)} \quad (8)$$

$$h_e = h_1 + h_2 \left[\frac{E_2}{E_1} \right]^{1/3} \quad (9)$$

where E_1 and E_2 are the current moduli of the AC and base layers, h_1 and h_2 the current thickness of AC and base and h_e is the equivalent thickness of AC needed to maintain the current stiffness of AC and base combined.

The following equations were used to calculate standard deviations (STD), and coefficients of

variation (V):

$$STD = \left[\frac{1}{n} \sum (x - MEAN)^2 \right]^{1/2} \quad (10)$$

$$V = \frac{STD}{MEAN} \quad (11)$$

where x is any variable examined, MEAN is the mean value of the variable and n is the number of samples.

The following equations were used to calculate the correlation coefficient ρ :

$$\rho = \frac{COV_{xy}}{STD_x STD_y} \quad (12)$$

where:

$$COV = \frac{1}{n} \sum (x - MEAN_x)(y - MEAN_y) \quad (13)$$

is the covariance of variables x and y, and STD_x and STD_y are standard deviations of the variables x and y, respectively.

ANALYSES

Three types of data analysis were performed: (a) variations defining initial pavement conditions; (b) variations of selected variables at different load repetitions; and (c) cross correlations of selected variables taken at different load repetitions. To carry out the analyses, first the statistics of the selected variables were calculated so as to detect the existence of differences in the structural capacity of the inner and outer track before trafficking; then, a check was made to see if and how any of these variables may have changed during trafficking; finally, cross correlations were performed to check the relative influence of initial pavement condition (thickness, strength, roughness etc.) on pavement performance. Actual test trafficking was started after the pavement had received approximately 20,000 repetitions of mixed loadings over the whole pavement. These loadings can be considered as conditioning cycles.

Odemark's concept was used to evaluate the variability of the different layers of the pavement in lieu of Layer Theory. The Odemark concept was selected because it was felt that using measured FWD deflection basins could induce a variety of errors in the modulus calculations (sometimes

called back calculations) and also since deflections away from load center reflect predominately subgrade influences. Since the distance from the bottom of the concrete trough to the point of FWD load application varies as FWD loads are applied at the surface of the subgrade, base, and AC layer and because total distance from the FWD sensors to trough bottom is less than 1.5 m, it was felt that load center deflections would be more meaningful and prone to less error when calculating moduli.

Also the term “displacement” has been used to denote the elastic displacement of the pavement or of the layers of the pavement occurring under load, specifically in this study, displacements to FWD loading. The term deformation is used as a measure of the deformed state of the pavements surface. At CAPTIF three different measures of the deformed state of the pavements surface were obtained (a) profile measured by dipstick or laser profilometer, (b) vertical surface deformation (VSD) taken from transverse measurements at each station referred to a fixed elevation, and (c) rut depth calculated from the VSD’s.

Variations Defining Initial Conditions

Spatial variations of parameters associated with the pavement’s structural integrity at construction were calculated so as to detect the existence of differences in the structural capacity of the inner and outer track prior to the actual trafficking of the pavements after 20,000 preload repetitions.

Spatial Variation of Layer Thickness at Construction: The thicknesses of the base and AC layers in each wheel path were measured during construction. Figures 1 and 2 are plots of layer thickness around the track and table 1 lists basic statistics derived from these data. The variation in layer thickness for the two top layers in both paths is small, between 4.3 percent and 7.7 percent. Mean thickness values, STD’s and V’s between the inner and outer tracks are similar. For both wheel paths the variation of AC thickness is about 75 percent greater than the variation of the base thickness as might normally be expected. Note the distinct occurrence of wavelengths between 10 m and 20 m (frequencies between 0.05 to 0.1 cycles/m) of base thickness in both tracks possibly due to hand leveling construction techniques. Over all, these findings indicate that the inner and outer wheel tracks are geometrically similar statistically.

Note: Cross-correlations conducted between base and AC layer thickness in each wheel path around the track reflect a trivial but interesting finding: the base and AC thicknesses are highly negatively correlated. The coefficients of cross-correlation are -0.803 for the inner and -0.789 for the outer wheel paths. This is a logical finding because during pavement construction, the surface layer is normally made as flat and as smooth as possible. Therefore, wherever the base layer is thicker, the AC layer is thinner and vice versa.

Spatial Variation of FWD Layer Deflections at Construction: FWD center deflections on the top of each layer were taken during construction. Unit load deflections for all layers plotted in figures 3 and 4 seem to vary quite randomly. Basic statistics given in table 2 show that the

variation of unit deflections for all layers in both wheel paths is about 10 percent. Although mean deflection on top of the AC layer of the outer path is about 7 percent less than that of the inner path (outer is stiffer), mean deflections at the top of base and subgrade for inner and outer wheel paths are about the same. All other statistics between inner and outer tracks are similar.

Subgrade deflection is in general 34 percent larger than base course deflection indicating that the base course does in fact tend to stiffen the overall pavement except at stations 16 and 37 where subgrade deflections on the outer wheel path were less than the base course deflections; indicating either a weaker base course in this area or data error. The overall findings, except for the reverse deflections found between subgrade and base at stations 16 and 37, all together indicate that the inner path at construction, was structurally similar to the outer path.

Spatial Variation of Layer Moduli at Construction: Layer moduli at 1-m intervals in each wheel path around the track were calculated using equations (3) through (7) and plotted in figures 5 and 6. Basic statistics are given in table 4.

Note: At stations 16 & 37, the subgrade deflection is higher than the base deflection. The higher subgrade deflections at stations 16 and 37 in the outer track were however not used in the Odemark method to calculate base and AC moduli because of the limits set by the method on deflections. At these two stations, it was thus decided to set subgrade modulus equal to base modulus.

It is also interesting that the coefficient of variation of subgrade modulus in each wheel path are of the same order of variation as is FWD deflection (10 percent) but the coefficients of variation for base (20 percent), and AC modulus (30 percent) are two and three times greater than the respective coefficients of variation for deflections. Since the coefficient of variation for moduli of the base and surface should be of the same order as the coefficient of variation for deflection, we see that the error induced is generated by the use of Boussinesq and Odemark method when estimating layer modulus, and that it depends upon the number of layers input into the back calculation process.

Spatial Variation of Initial Equivalent Stiffness at Construction: The combined equivalent stiffness of the AC and base layers was calculated at every meter around the track in both wheel paths using equations (8) and (9) and are shown in figure 7. Basic statistics of the equivalent stiffness are listed in table 5. The mean equivalent stiffness of the upper two layers of the outer track is about 10 percent greater than that of the inner track (note mean deflections were 10 percent less). The small 10 percent difference between inner and outer track indicates comparable structural condition of the combined effect of the upper layers. Variation of the equivalent stiffness in both tracks is about the same 20 percent but it should probably be on the order of 10 percent in keeping with the finding above, that the induced error in the coefficient of variation is additive.

Spatial Variation of FWD Deflections at Beginning of Test (after preloading): Since a lengthy

period of time had elapsed between final construction and the start of testing after the 20,000 conditioning cycles, it is important to again compare the structural integrities of the two wheel paths. The FWD surface deflections for both inner and outer tracks at 20-k load repetitions (beginning of trafficking) are plotted in figure 8a and basic statistics listed in table 3. The mean values of surface deflection indicate that generally the structural integrity of the inner and outer pavements are still very similar after preloading but note that the coefficients of variation V differ slightly: 9.4 percent for inner track (was 9.3) and 11.5 percent for outer track using all data (before any loading was 10.1 percent). This small difference is largely due to the fact that at station 21, the surface deflection of the outer track is about 30 percent higher than its mean value (maximum is about 15 percent more than its mean at some other location in the pavement) indicating that the outer pavement is relatively weaker than the inner track around stations 21. Figures 8b and 8c are comparisons of the change in deflection from construction to start of testing. The change in the structural integrity is obvious at station 21 as seen in figure 8c for the outer track.

Correlation between FWD Surface Deflections at Beginning of Test : Since we are more interested in transverse uniformness, it is crucial that transverse variability be minimized. In order to obtain a clearer understanding of the significance in the higher deflections at station 21, we conducted cross correlations between inner and outer deflections using the deflections at all 58 stations around both inner and outer tracks and similarly using these data less the deflections occurring between stations 18 and 24 (SELECT data). The correlation coefficients obtained, 0.61 using ALL data and 0.81 using SELECT, suggest a 33 percent increase in the correlation between the two pavements when the weak section is not considered. The higher correlation indicates that the two tracks are very similar before trafficking at 20,000 cycles. Note also in table 3 that if we use SELECT deflection data for outer and ALL deflection data for the inner tracks, the mean deflections 0.949 for the inner and 0.945 for outer; and the STD's 0.0941 for inner and 0.0978 for outer tracks are in deed almost identical values.

Variations of Selected Variables at Different Load Repetitions

Variations of selected variables at different load repetitions during trafficking were calculated to see how these parameters may have changed.

Dynamic Load Coefficient (DLC) and International Roughness Index (IRI): The static load on each suspension in each wheel path was identical and was kept constant throughout testing. The only reason for differences in the vertical dynamics between the two tracks is due to the roughness in each lane and the dynamic effects caused by the different frequencies and stiffness of the suspensions; air suspension operating on the inner and steel suspension on the outer track. The dynamic component of loading is identified by the dynamic load coefficient called DLC (defined as standard deviation divided by the mean load). The DLC's of the steel and air suspensions were calculated at different load repetitions are plotted in figure 9. The DLC of the steel suspension is initially about 350 percent times greater than air but drops suddenly between 20,000 and 60,000 cycles. It then increases and remains between 3.5 and 4 times greater than air.

Both DLC's drop similarly at 20,000 cycles , about 80 percent for steel and 70 percent for air.

Note: Since the IRI's are initially close to the lowest IRI values attained (at 80,000 repetitions), the drop in DLC's cannot be attributed to "high initial IRI". Although the IRI on the outer track is initially lower than the IRI of the inner track (DLC's higher), both IRI's become basically the same.

Profiles - Wheel path centerline elevations (profiles) and elevation changes taken at selected times during trafficking are plotted versus distance around the inner and outer tracks in figures 10 and 11. General statistics pertaining to these data are summarized in tables 6. We see from this information that between 20-k and 200-k load repetitions, a large unexpected surface depression (rut) occurred between stations 18 and 24 on the outer track, the same area experiencing the larger FWD displacements before trafficking. If the rut is to be considered as a localized construction failure, then one would have expected FWD surface deflections to be high at or around station 21 at the completion of construction but that was not the case. However after preloading (20-k random vehicle loadings), the deflections around station 21 did increase from about 10 percent less than the mean at construction to about 30 percent higher than the mean at 20-k load repetitions. There is no explanation on how this happened. One possible explanation for the rut is that some how water got into the outer edge of the test track and changed the local moisture content of the subgrade thus dramatically changing the stiffness of the pavement around that region.

Because it is logical that the rut is attributed to a weakened pavement condition in the outer track around station 21 and not to dynamic loading in general, it was reasoned that the analysis for the outside track should be conducted using data that did not contain the rut (SELECT data), as well as with data containing the rut (ALL data). It was also reasoned that the analysis of the inner track in many cases should be primarily conducted using ALL data since the inner track contained no obvious "outlier." Throughout the analysis, we have attempted to identify when and why ALL or SELECT data were used.

As shown in table 6 and figure 11c, using ALL data, mean profile change between 20-k and 1700-k repetitions on the inner track is 8 mm and the mean profile change on the outer track between 20-k and 1700-k repetitions using ALL data is 13 mm; thus the change in mean profile on the outer track using ALL data is about 61 percent greater than that on the inner track. One might be tempted to consider these changes in mean elevation as being due to dynamic loading, but since the tires on the inner and outer tracks are under the same static load, then theoretically the change in mean elevation should be the same for any value of dynamic loading considering that the two wheel paths are very similar. The fact that the mean elevation changes are not the same in both tracks is most likely due to the errors induced by using the dipstick measurement technique.

From table 6, the change in the coefficient of variation, V , of the profile elevations (from beginning to end) is 14 percent on the inner track and is 33 percent on the outer track using ALL.

data for both tracks. One could infer from this that the steel suspension has caused a roughness change that is about 19 percent greater than the roughness change caused by the air suspension.

Vertical Surface Deformation (VSD) Vertical Surface Deformation (VSD) is calculated from data measured transversely at each station using a fixed reference beam on both tracks. Because these measurements are in concert with the stations around the track and because there is little chance of any induced error with respect to the magnitudes of the elevations being recorded, it was determined these measurements should be used in the analyses in lieu of the measurements taken with the dip stick. Table 7 shows that the change in mean VSD, between 20-k and 1700-k repetitions on the outer track is actually 9.67 percent smaller (using SELECT and ALL data on outer and inner tracks respectively) than the change on the inner track. This indicates that dynamic loading has no effect on the accumulation of mean surface deformation. Figure 12d is a plot of the rate of change of mean VSD (using ALL data for both pavements). This shows that the changes in the two pavements are almost identical after early loading. This further confirms once again that the dynamic wheel force had no effect on the change in mean VSD.

If we look at the change in the standard deviation of VSD, between 20-k and 17000-k, it is seen that the change in the standard deviation of VSD on the outer track is 26.3 percent greater than that on the inner track using SELECT and ALL data for the outer and inner tracks respectively.

If we look at the coefficient of variation of VSD at the end of test, it is seen that the coefficient of variation of VSD on the outer track is 27.7 percent greater than that on the inner track using SELECT data for both pavement tracks. Since the coefficient of variation of the FWD deflections on the outer track (from table 3) is 4 percent greater than that on the inner track, then it is sufficient to say that the steel suspension acting on the outer track is responsible for an overall 23.7 percent increase of the coefficient of variation of VSD. This increase can be interpreted as an increase in pavement roughness due to dynamic loading.

Cross correlations between inner and outer track VSD at different load repetitions are plotted in figure 12e. The low values of correlation means that pavement surface roughness is different between the two tracks initially and that it remains different throughout trafficking. When the rut is included in the outer track, there is a negative correlation suggesting that the rut is so significant that the correlation of the variables around station 21 dominate the whole data set.

Rut Depth - Figure 13a is a plot of mean rut depth versus load cycles using ALL and SELECT data. The SELECT data sets show similar mean rut depth behavior throughout trafficking between inner and outer tracks but when ALL data is used for the outer track, mean rut depth in the outer track is about 13 percent greater than that on the inner track again reflecting the influence of the localized rut failure at station 21 on the outer track. From table 8 using SELECT data for the outer and ALL data for the inner, the change in mean rut on the outer track is actually 3.9 percent less than the change on the inner again confirming that dynamic loading has no positive effect on the accumulation of mean rut depth. Figure 14d is a plot of the rate of change

of mean rut depth. This shows that the rate of change in rut depth in the two pavements is similar after early loading using ALL data. This further confirms once again that the dynamic wheel force did not affect average pavement rut depth.

Figure 13b is a plot of the ratio of the coefficients of variation of outer to inner track rut depths using SELECT data. It is seen that there is a gradual increase in the variability of the outer track when compared to the inner track, from about -13 to about +20 percent (when ALL data is used for the inner and SELECT for the outer, then slightly lower values are attained). This overall increase in the variability of rutting in the outer track can be attributed to the dynamic forces induced by the steel suspension.

If we look at the coefficient of variation of rut depth at the end of test, it is seen that the coefficient of variation of rut depth on the outer track is 19 percent greater than the coefficient of variation of rut depth on the inner using SELECT data on both tracks. This further confirms that the steel suspension on the outer track was responsible for 15 percent (19 percent minus 4 percent) more rutting damage in the outer track.

Cross correlations between inner and outer rut depth at different load repetitions are plotted in figure 14e. The low values of correlation indicate that the pavement surface profiles are different initially and remain different throughout trafficking. When the rut is included in the analysis there is negative correlation of rutting between the inner and outer tracks indicating that the rut is very significant in the correlation analysis.

Cross Correlation

Linear and nonlinear cross correlations at different load repetitions among the variables, FWD surface deflection, profile elevation, VSD, rut depth, cracking, and wheel force, were calculated in an attempt to determine the degree of correlation between these variables and the possibility of the existence of a relationship between these variables. Calculations using ALL data and SELECT data were made. A more complete picture of the effects of dynamic loading and variability on pavement performance can thus be attained using these techniques.

Linear Cross Correlations between Initial Variability and Performance Measures.

The coefficient of correlation determined from a cross correlation between two variables X_1 and X_2 , may be thought of as a measure of the degree of influence of one variable on the other. For instance, if the coefficient of correlation between X_1 and X_2 is 1.0, then a linear relationship between these two variables is said to exist; in this case, the perfect relationship that exists between the variables X_1 and X_2 dictates that these two variables are dependent one on the other. If the coefficient of correlation is zero, then the occurrence of X_1 has no influence on the occurrence of X_2 ; in this case, we must rely on other variables $X_3 \dots X_n$ to explain the occurrence of variables X_1 and X_2 .

1. FWD SURFACE DEFLECTION and VSD- Coefficients of correlation between FWD surface deflections measured at 20-k repetitions and VSD's measured at different repetitions using ALL data for inner and SELECT data for outer tracks are plotted in figure 15. The positive correlations represented by these curves indicate that the VSD's of both the inner and outer tracks can be explained by the FWD deflections at 20-k repetitions such that initially weaker pavements portions generate higher VSD's. A lower correlation means that VSD is explained less by initial stiffness and more by other factors. It is evident from these curves where the coefficient of correlation for the inner track is about 0.75 and for the outer track is about 0.3, that factors other than pavement stiffness, namely dynamic loads, played a bigger role in explaining VSD in the outer track (because of the lower correlation) than they did for the inner track.

2. FWD SURFACE DEFLECTION and RUTTING - Coefficients of correlation between FWD surface deflection at 20 k and rut depth are shown in figure 16. The difference between inner and outer tracks is much smaller than the correlation between FWD deflection at 20 k and VSD. This may be explained by the fact that VSD is an absolute measure of vertical deformation referred to a fixed elevation and that rut depth is the vertical deformation at the center of the wheel path relative to the pavement surface. Since the rut depths for the inner and outer tracks are similar (if the rut at station 21 in the outer track is excluded), the correlation between the two tracks are similar.

3. FWD SURFACE DEFLECTION and CRACKING - To examine the effect of pavement structural variation on pavement surface cracking, cross correlations between pavement surface cracking (total, longitudinal and transverse) and FWD surface deflection were calculated. It is shown (see figures 17a to 17c) that the correlation coefficients for outer track are about 0.7 indicating moderate correlation between cracking and pavement initial structural conditions. For the inner track, coefficients of 0.5 were obtained. The fact that there is poorer correlation on the inner track indicates that other factors, such as shearing stresses, have greater change affecting cracking on the inner track. The possibility of non linear effects is discussed below.

Note: If we use ALL data, the correlation coefficients are about 0.5-0.6 for both inner and outer tracks.

Linear Cross Correlations between Wheel Force and Other Variables

1. WHEEL FORCE and FWD SURFACE DEFLECTION - Figure 18 shows the coefficient of correlation between wheel force and surface deflections at the beginning of the test. As it would normally be expected, the low correlation supports the assumption that variation of pavement stiffness does not influence dynamic wheel forces in flexible pavements.

2. WHEEL FORCE and VSD - The correlation between wheel force and VSD as a function of load repetitions is plotted in figure 19. It is interesting to note that the inner track showed a negative correlation while the outer track showed a positive correlation. However, both

correlations are rather weak. The weak correlations between VSD and wheel force would be expected in light of the stronger correlations between FWD surface deflection.

3. WHEEL FORCE and SURFACE CRACKING - Similarly to what was obtained from the linear cross correlations between wheel force and pavement rutting, correlations between wheel force and surface cracking are very weak (see figures 20a through 20c).

Linear Cross Correlation between Cracking and Rut Depth

Linear cross correlation analysis between surface cracking and rut depth was conducted using ALL data for both outer and inner tracks at different load repetitions. Coefficients of correlation of about 0.8 for the outer and about 0.4 for the inner track are shown plotted in figures 21a and 21b. The moderate correlation for the outer track indicates that more cracking damage is associated where the location of rutting is more severe.

Linear Cross Correlation between Final (1700-k) Profile and Profiles at other Load Repetitions

Coefficients of correlation between profile at the end of test (1700-k repetitions) and profiles taken at different load repetitions are shown in figures 22. The results confirm that after 400-k load repetitions, the profiles change similarly at different load repetitions and that the initial profile has little influence on the final profiles of the two tracks regardless of the type of suspension.

Pseudo Nonlinear Cross Correlations between VSD and Other Variables

In order to further examine the existence of any relationship among the variables, wheel force, VSD, and FWD surface deflection, these data were manipulated in various ways and their cross correlations were calculated.

1. VSD AND WHEEL FORCE* SURFACE DEFLECTION - This correlation yields the curves plotted in figure 23. It can be seen that when wheel force is combined with the initial structural condition, the correlation between wheel force and VSD becomes much stronger, however, this is mainly attributed to pavement structural condition rather than wheel force.

Note: The physical meaning of the product of wheel force and deflection is the work done by the vehicle.

2. VSD and WHEEL FORCE/ SURFACE DEFLECTION - This correlation yields a stronger but negative correlation for the inner track (see figure 24). The linear cross correlation between wheel force and VSD was stronger for the outer track when compared with the inner track. It may be interpreted that for the outer track, 30 percent of the VSD is attributed to structural variability and 40 percent to the steel suspension. For the inner track, about 70 percent of the VSD is attributable to structural variability.

Pseudo Nonlinear Cross Correlation between Wheel Force and other Variables

WHEEL FORCE and VSD^M/FWD SURFACE DEFLECTION - The correlation coefficients of variables VSD^M/FWD and wheel force as a function of load repetitions are plotted in figures 25a through 25c for both inner and outer tracks. It can be seen that as load repetitions increase, the steel suspension affects VSD more than the air suspension. We can speculate that the steel suspension explains about 40 percent of the accumulated VSD while the influence from the air suspension is very weak (-0.2 to +0.1). The correlation coefficients obtained when the exponent M takes on positive values are also given in figures 25. The results show that the strongest correlation is obtained when $M = 1/3$. This correlation implies that 50 percent of the VSD on the outer track can be explained by the steel suspension, and that the wheel force of the air suspension has little or no influence on VSD.

WHEEL FORCE and VSD/FWD³ - The correlation coefficients of wheel force and VSD/FWD³ as a function of load repetitions are plotted in figures 26a and 26b for both inner and outer tracks using ALL data and SELECT data, respectively. The similar correlation can be observed as it exists between wheel force and VSD^{1/3}/FWD. It confirms that the structural variability indeed plays an importance role in the development of VSD and the steel suspension affects VSD more than the air suspension. Based on this cross correlation analysis, it is therefore further conclude that the steel suspension explains about 60 percent of the accumulated VSD while the wheel force of the air suspension has little or no influence on VSD if the effect of pavement structural variability is excluded.

Pseudo Nonlinear Cross Correlation between Performance Measures and other Variables

The analysis herein is an attempt to determine the best fit relationship expressing the pavement performance measures VSD and profile, considered as dependent variables, in terms of and FWD surface deflection and dynamic wheel force (WF), considered as independent variables. The following relationships for VSD were assumed:

1. $VSD = b * FWD^{P1}$
2. $VSD = a * WF^{P2}$
3. $VSD = c * FWD^{P1} * WF^{P2}$
4. $VSD = FWD^{P1} * WF^{P2} * N^{P3}$
5. $VSD = b * FWD^{P1} + a * WF^{P2} + c * FWD^{P1} * WF^{P2}$

where a, b, and c are coefficients, P1, P2 and P3 are exponents and N is number of load repetitions, and WF is the average of wheel forces at two different load cycles, e.g. $(WF(20\text{ k}) + WF(1700\text{ k}))/2$ and $(WF(500\text{ k}) + WF(1700\text{ k}))/2$.

Regression analysis results for the above assumed VSD relationships are listed in table 9 along with the analysis results for the profile. In the case of the profile, the dipstick value closest to a given station was used. The results once again confirm that initial pavement structural condition

influences pavement performance more than other factors. Based on the results, it appears that

- The best relationship for VSD is

$$\text{VSD} = c * \text{FWD}^{P1} * \text{WF}^{P2}$$

which yielded coefficients of correlation of 0.54 for the inner track (with $P1=1.005$ and $P2=0.225$) and 0.759 for the outer track (with $P1=3.222$ and $P2=1.781$).

- The best relationship for profile is

$$\text{Profile} = b * \text{FWD}^{P1} + a * \text{WF}^{P2} + c * \text{FWD}^{P1} * \text{WF}^{P2}$$

which yielded coefficients of correlation of 0.639 for the inner track (with $P1=0.502$ and $P2=1.079$) and 0.667 for the outer track (with $P1=0.011$ and $P2=2.967$).

CONCLUSIONS

Based on these analyses, the following conclusions are drawn:

1. The thickness of the top layer and base layer of the test pavement is highly negatively correlated because of the intent to make the pavement surface flat and smooth.
2. There is little difference between the structural integrity of both wheel paths at construction. However, an increase in FWD surface deflections around station 21 (between stations 18 and 24) on the outer track, taken just prior to test trafficking (at 20-k repetitions) indicated that the pavement had weakened in that area:
 - A rut occurred on the outer track (steel suspension) between stations 18 and 24 during the initial stages of trafficking, and because of the high FWD deflections, rutting in that area is believed to be due to localized pavement conditions.
 - Because of the rut on the outer track, two sets of data: SELECT data (data set not containing the rut) and ALL data (data set containing the rut) were used in the analysis. In most cases, SELECT data were used for the outside track analyses whereas for the inner track both ALL data and SELECT data were used since the inner track contained no obvious localized "outlier."
3. At the end of testing, there was no change in mean vertical surface deformation (VSD) nor in mean rut depth, indicating that dynamic loading had little or no effect on the accumulation of mean surface deformation.

4. Comparisons of the change in roughness between the two tracks were made:

- At the end of testing, the coefficient of variation of VSD on the outer track is 27.7 percent greater than that on the inner track using SELECT data for both tracks. Since the coefficient of variation of the FWD deflections on the outer track is 4 percent greater than that on the inner track, this leads to the finding that the steel suspension was responsible for overall 23.7 percent (27.7 percent - 4.0 percent) more roughness damage on the outer track based on VSD measurements.
- At the end of testing, the coefficient of variation of rut depth on the outer track was 19 percent greater than the coefficient of variation of rut depth on the inner track using SELECT data for both tracks. This confirms that the steel suspension was responsible for overall 15 percent (19 percent - 4 percent) more surface roughness damage on the outer track based on rut depth measurements.
- The change in the coefficient of variation of the profile elevations is 14 percent on the inner track and 33 percent on the outer track using ALL data for both tracks, indicating that the steel suspension has caused a roughness change about 19 percent greater than that caused by the air suspension based on surface profile measurements.

5. Cross correlation between surface cracking and rutting yielded coefficients of correlation of 0.8 for the outer and 0.4 for the inner track. Given that the mean rut depths of the two tracks are similar, the greater variation of rut depth on the outer track dictates the existence of more locations with more rutting around the track; the higher correlation on the outer track indicates that surface cracking started when rutting reached a certain level of severity. Therefore, it may be concluded that the steel suspension induced wheel force caused more localized rutting damage, thus more cracking.

6. The initial profile had little influence on the final profile in the two different tracks regardless of the type of suspension.

7. Linear and nonlinear relationships among FWD surface deflection, profile elevation, VSD, rut depth, cracking and wheel force were analyzed in an attempt to determine the degree of correlation between these variables. It was found that:

- The coefficient of correlation between VSD and FWD surface deflection for the inner track is about 0.75 and for the outer track about 0.3. The stronger correlation on the inner track indicates that pavement variability played a more dominant role in explaining the occurrence of VSD on the inner track. The poorer correlation on the outer track indicates that factors other than pavement variability, such as load, played a bigger role in explaining VSD on the outer track.
- The coefficients of correlation between rut depth and FWD surface deflection for both tracks

are similar around 0.6. This could be attributed to the way which the rut depth was determined, i.e. the difference between the highest and lowest surface elevation for any given cross pavement section.

- The coefficient of correlation between wheel force and VSD, normalized by FWD surface deflection, for the inner track is about -0.2 and for the outer track about 0.4. The stronger correlation for the outer track indicates that wheel force plays a bigger role in explaining VSD on the outer track. This could be interpreted that 40 percent of the VSD is attributed to the dynamic wheel force generated by the steel suspension and that dynamic wheel force generated by the air suspension had little influence on VSD. This statement can be made in light of the fact that structural variability is eliminated from the correlation analysis.
- The coefficient of correlation between wheel force and the cubic root of VSD, normalized by FWD, is about 0.1 for inner track and 0.5 for outer track. The stronger correlation for the outer track indicates that wheel force plays a bigger role in explaining VSD on the outer track. This could be interpreted that 50 percent of the powered VSD is attributed to the steel suspension induced dynamic wheel force and that the air suspension induced dynamic force had very little or no influence on VSD.
- The coefficient of correlation between wheel force and VSD, normalized by FWD to the power of 3, showed similar results as above - about 0.6 for the steel suspension and 0.2 for the air suspension. This result implies that about 60 percent of the VSD on the outer track can be explained by the steel suspension induced dynamic wheel force and the dynamic wheel force induced by air suspension has little or no influence on VSD.
- Other nonlinear correlation analyses among the variables, profile, VSD, wheel force, and surface deflection were also conducted and the best fit relationships were determined, however, similar or lower coefficients of correlation were obtained.

Table 1. Statistics of CAPTIF Pavement Layer Thickness

	MEAN	MINIMUM	MAXIMUM	STD	V
Outer Track					
H_{AC} (mm)	88	73	103	6.808	0.077
H_{base} (mm)	199	173	215	9.496	0.048
Inner Track					
H_{AC} (mm)	87	75	103	6.333	0.073
H_{base} (mm)	198	177	212	8.580	0.043

Table 2. Statistics of CAPTIF Pavement Unit Layer Deflection at Construction (FWD Data)

	MEAN	MINIMUM	MAXIMUM	STD	V
Outer Track					
AC (mm/kPa)	0.888	0.703	1.121	0.090	0.101
Base (mm/kPa)	1.742	1.309	2.099	0.179	0.103
Subgrade (mm/kPa)	2.383	1.674	2.737	0.224	0.094
Inner Track					
AC (mm/kPa)	0.954	0.748	1.135	0.089	0.093
Base (mm/kPa)	1.793	1.267	2.105	0.169	0.094
Subgrade (mm/kPa)	2.478	1.959	2.954	0.205	0.083

Table 3. Statistics of CAPTIF Pavement Unit Surface Deflection at Beginning of Test (at 20 k, FWD Data)

	MEAN	MINIMUM	MAXIMUM	STD	V
Inner Track					
All Data (mm/kPa)	0.949	0.768	1.095	0.089	0.094
Select Data (mm/kPa)	0.953	0.768	1.095	0.091	0.095
Outer Track					
All Data (mm/kPa)	0.965	0.796	1.258	0.111	0.115
Select Data (mm/kPa)	0.945	0.796	1.131	0.092	0.098

Table 4. Statistics of CAPTIF Pavement Layer Modulus

	MEAN	MINIMUM	MAXIMUM	STD	V
Outer Track					
E_{AC} (MPa)	1081.810	330.000	2183.000	404.780	0.374
E_{base} (MPa)	226.020	131.000	354.000	51.260	0.227
$E_{subgrade}$ (MPa)	106.710	92.000	151.000	11.120	0.100
Inner Track					
E_{AC} (MPa)	904.900	538.000	1658.000	262.550	0.290
E_{base} (MPa)	220.350	140.000	437.000	55.810	0.253
$E_{subgrade}$ (MPa)	102.340	85.000	129.000	8.680	0.085

Table 5. Statistics of CAPTIF Pavement Equivalent Stiffness

	MEAN	MINIMUM	MAXIMUM	STD	V
Outer Track					
Equivalent Stiffness (MPa·mm ³)	853900000	435800000	1343000000	187800000	0.220
Inner Track					
Equivalent Stiffness (MPa·mm ³)	768600000	567500000	1247000000	147400000	0.192

Table 6. Statistics of Pavement Elevation (Profile, m)

Load Repetition	Track	Data Set	Mean	Minimum	Maximum	STD	V	V_{outer}/V_{inner}
20 k	Inner	All Data	50.216	50.208	50.228	0.004	0.00007	
		Select Data	50.215	50.208	50.228	0.004	0.00008	
	Outer	All Data	50.219	50.211	50.229	0.004	0.00009	1.146
		Select Data	50.219	50.211	50.227	0.004	0.00007	0.960
60 k	Inner	All Data	50.215	50.208	50.228	0.004	0.00007	
		Select Data	50.215	50.208	50.228	0.004	0.00008	
	Outer	All Data	50.213	50.207	50.220	0.003	0.00006	0.861
		Select Data	50.214	50.208	50.220	0.003	0.00006	0.781
100 k	Inner	All Data	50.213	50.206	50.227	0.004	0.00008	
		Select Data	50.213	50.206	50.227	0.004	0.00008	
	Outer	All Data	50.211	50.198	50.218	0.004	0.00008	1.103
		Select Data	50.212	50.206	50.218	0.003	0.00006	0.766
200 k	Inner	All Data	50.212	50.205	50.225	0.004	0.00007	
		Select Data	50.212	50.205	50.225	0.004	0.00007	
	Outer	All Data	50.211	50.195	50.219	0.005	0.00010	1.361
		Select Data	50.213	50.207	50.219	0.003	0.00006	0.817
500 k	Inner	All Data	50.209	50.202	50.223	0.004	0.00008	
		Select Data	50.209	50.202	50.223	0.004	0.00007	
	Outer	All Data	50.208	50.189	50.217	0.006	0.00011	1.501
		Select Data	50.209	50.202	50.217	0.003	0.00007	0.908
1000 k	Inner	All Data	50.208	50.199	50.222	0.004	0.00008	
		Select Data	50.208	50.199	50.222	0.004	0.00008	
	Outer	All Data	50.207	50.187	50.217	0.006	0.00012	1.511
		Select Data	50.208	50.202	50.217	0.003	0.00007	0.863
1500 k	Inner	All Data	50.209	50.199	50.223	0.004	0.00008	
		Select Data	50.208	50.199	50.223	0.004	0.00008	
	Outer	All Data	50.205	50.184	50.215	0.006	0.00012	1.518
		Select Data	50.207	50.200	50.215	0.003	0.00007	0.817
1700 k	Inner	All Data	50.208	50.223	50.198	0.004	0.00008	
		Select Data	50.208	50.223	50.198	0.004	0.00008	
	Outer	All Data	50.204	50.215	50.181	0.006	0.00012	1.530
		Select Data	50.206	50.215	50.198	0.003	0.00006	0.827

Table 7. Statistics of Pavement Vertical Surface Deformation (VSD, mm)

Load Repetition	Track	Data Set	Mean	Minimum	Maximum	STD	V	V_{outer}/V_{inner}
20 k	Inner	All Data	0.710	-0.7	3.0	0.715	1.006	
		Select Data	0.754	-1.0	3.0	0.736	0.976	
	Outer	All Data	0.750	-0.7	3.0	0.714	0.952	0.946
		Select Data	0.781	-1.0	3.0	0.718	0.920	0.942
60 k	Inner	All Data	2.760	1.0	5.0	0.722	0.262	
		Select Data	2.821	1.0	5.0	0.683	0.242	
	Outer	All Data	3.197	1.0	13.1	2.515	0.787	3.007
		Select Data	2.440	1.0	5.0	0.798	0.327	1.350
100 k	Inner	All Data	5.078	3.0	7.0	1.129	0.222	
		Select Data	5.196	3.0	7.0	1.072	0.206	
	Outer	All Data	5.748	2.0	22.3	4.188	0.729	3.276
		Select Data	4.473	2.0	7.0	1.220	0.273	1.322
200 k	Inner	All Data	6.128	4.0	9.0	1.252	0.204	
		Select Data	6.285	4.0	9.0	1.196	0.190	
	Outer	All Data	7.157	3.0	27.5	5.058	0.707	3.459
		Select Data	5.614	3.0	9.0	1.196	0.213	1.119
500 k	Inner	All Data	8.366	5.3	11.7	1.528	0.183	
		Select Data	8.564	5.0	11.7	1.470	0.172	
	Outer	All Data	9.407	4.0	32.0	5.864	0.623	3.413
		Select Data	7.614	4.0	11.2	1.627	0.214	1.245
1000 k	Inner	All Data	8.857	5.6	12.8	1.775	0.200	
		Select Data	9.087	6.0	12.8	1.711	0.188	
	Outer	All Data	10.157	4.4	34.0	6.174	0.608	3.034
		Select Data	8.275	4.0	12.7	1.846	0.223	1.185
1500 k	Inner	All Data	9.557	5.9	13.4	1.843	0.193	
		Select Data	9.762	6.0	13.4	1.807	0.185	
	Outer	All Data	10.971	5.3	35.8	6.456	0.588	3.052
		Select Data	9.010	5.0	13.6	1.972	0.219	1.183
1700 k	Inner	All Data	9.688	6.2	13.7	1.879	0.194	
		Select Data	9.915	7.0	13.7	1.814	0.183	
	Outer	All Data	10.835	4.7	35.9	6.500	0.600	3.093
		Select Data	8.887	5.0	14.0	2.076	0.234	1.277

Table 8. Statistics of Pavement Rut Depth (mm)

Load Repetition	Track	Data Set	Mean	Minimum	Maximum	STD	V	V_{outer}/V_{inner}
20 k	Inner	All Data	1.428	0.0	4.8	1.139	0.798	
		Select Data	1.385	0.0	4.8	1.102	0.796	
	Outer	All Data	1.433	-0.6	4.5	0.967	0.675	0.846
		Select Data	1.398	-1.0	4.5	0.968	0.692	0.870
60 k	Inner	All Data	2.929	1.0	5.7	1.108	0.378	
		Select Data	2.983	1.0	5.7	1.069	0.358	
	Outer	All Data	3.388	1.0	13.8	2.537	0.749	1.980
		Select Data	2.640	1.0	4.6	0.932	0.353	0.985
100 k	Inner	All Data	4.993	3.0	7.6	1.211	0.243	
		Select Data	5.110	3.0	7.6	1.169	0.229	
	Outer	All Data	5.966	3.0	23.8	4.243	0.711	2.932
		Select Data	4.662	3.0	7.3	1.081	0.232	1.013
200 k	Inner	All Data	5.871	3.0	8.5	1.299	0.221	
		Select Data	6.008	4.0	8.5	1.237	0.206	
	Outer	All Data	7.269	3.1	29.0	5.344	0.735	3.322
		Select Data	5.614	3.0	8.6	1.226	0.218	1.060
500 k	Inner	All Data	7.712	4.2	10.8	1.528	0.198	
		Select Data	7.898	5.0	10.8	1.428	0.181	
	Outer	All Data	9.279	3.5	33.2	6.005	0.647	3.266
		Select Data	7.433	4.0	11.3	1.570	0.211	1.169
1000 k	Inner	All Data	8.214	4.7	11.7	1.752	0.213	
		Select Data	8.423	5.0	11.7	1.660	0.197	
	Outer	All Data	9.805	3.5	35.2	6.384	0.651	3.053
		Select Data	7.852	4.0	13.2	1.868	0.238	1.208
1500 k	Inner	All Data	8.650	5.1	12.6	1.883	0.218	
		Select Data	8.814	5.0	12.6	1.842	0.209	
	Outer	All Data	10.419	3.6	37.1	6.770	0.650	2.985
		Select Data	8.350	4.0	14.2	2.064	0.247	1.183
1700 k	Inner	All Data	8.753	5.2	12.4	1.817	0.208	
		Select Data	8.935	6.0	12.4	1.738	0.195	
	Outer	All Data	10.459	3.7	36.9	6.623	0.633	3.050
		Select Data	8.439	4.0	14.0	1.953	0.231	1.190

Table 9. Correlation between Assumed CAPTIF Test Pavement Performance Models and Measured Data

Equation	Load Repetition	Track	r Profile Changes	r VSD
Profile= $a \cdot WF^{P2}$ VSD= $a \cdot WF^{P2}$	1700 k-20 k	Inner	0.296 ($P_2=1.524$)	0.243 ($P_2=1.102$)
		Outer	0.204 ($P_2=0.656$)	0.314 ($P_2=1.225$)
	1700 k-500 k	Inner	0.054 ($P_2=0.878$)	0.062 ($P_2=0.983$)
		Outer	0.182 ($P_2=0.338$)	0.237 ($P_2=0.799$)
Profile= $b \cdot FWD^{P1}$ VSD= $b \cdot FWD^{P1}$	1700 k-20 k	Inner	0.627 ($P_1=1.483$)	0.533 ($P_1=1.105$)
		Outer	0.534 ($P_1=2.083$)	0.603 ($P_1=3.060$)
	1700 k-500 k	Inner	0.160 ($P_1=1.200$)	0.113 ($P_1=0.714$)
		Outer	0.459 ($P_1=1.596$)	0.312 ($P_1=2.024$)
Profile= $c \cdot FWD^{P1} \cdot WF^{P2}$ VSD= $c \cdot FWD^{P1} \cdot WF^{P2}$	1700 k-20 k	Inner	0.629 ($P_1=1.429$ $P_2=0.225$)	0.535 ($P_1=1.005$ $P_2=0.225$)
		Outer	0.626 ($P_1=2.429$ $P_2=1.072$)	0.759 ($P_1=3.222$ $P_2=1.781$)
	1700 k-500 k	Inner	0.161 ($P_1=1.152$ $P_2=0.321$)	0.117 ($P_1=0.648$ $P_2=0.423$)
		Outer	0.532 ($P_1=1.683$ $P_2=0.491$)	0.404 ($P_1=1.172$ $P_2=0.781$)
Profile= $FWD^{P1} \cdot WF^{P2} \cdot N^{P3}$ VSD= $FWD^{P1} \cdot WF^{P2} \cdot N^{P3}$	1700 k-20 k	Inner	0.629 ($P_1=1.429$ $P_2=0.225$)	0.535 ($P_1=1.005$ $P_2=0.225$)
		Outer	0.626 ($P_1=2.429$ $P_2=1.072$)	0.759 ($P_1=3.222$ $P_2=1.781$)
	1700 k-500 k	Inner	0.161 ($P_1=1.152$ $P_2=0.321$)	0.117 ($P_1=0.648$ $P_2=0.423$)
		Outer	0.532 ($P_1=1.683$ $P_2=0.491$)	0.451 ($P_1=2.273$ $P_2=1.071$)
Profile= $a \cdot FWD^{P1} + b \cdot WF^{P2} + c \cdot FWD^{P1} \cdot WF^{P2}$ VSD= $a \cdot FWD^{P1} + b \cdot WF^{P2} + c \cdot FWD^{P1} \cdot WF^{P2}$	1700 k-20 k	Inner	0.639 ($P_1=0.502$ $P_2=1.079$)	0.533 ($P_1=1.052$ $P_2=-9.055$)
		Outer	0.667 ($P_1=0.011$ $P_2=2.967$)	0.723 ($P_1=2.214$ $P_2=0.00004$)
	1700 k-500 k	Inner	0.165 ($P_1=0.471$ $P_2=0.978$)	0.117 ($P_1=0.634$ $P_2=1.337$)
		Outer	0.569 ($P_1=0.065$ $P_2=2.217$)	0.461 ($P_1=0.0005$ $P_2=2.469$)

Note: a, b, and c are coefficient constants and P1, P2, and P3 are exponents.

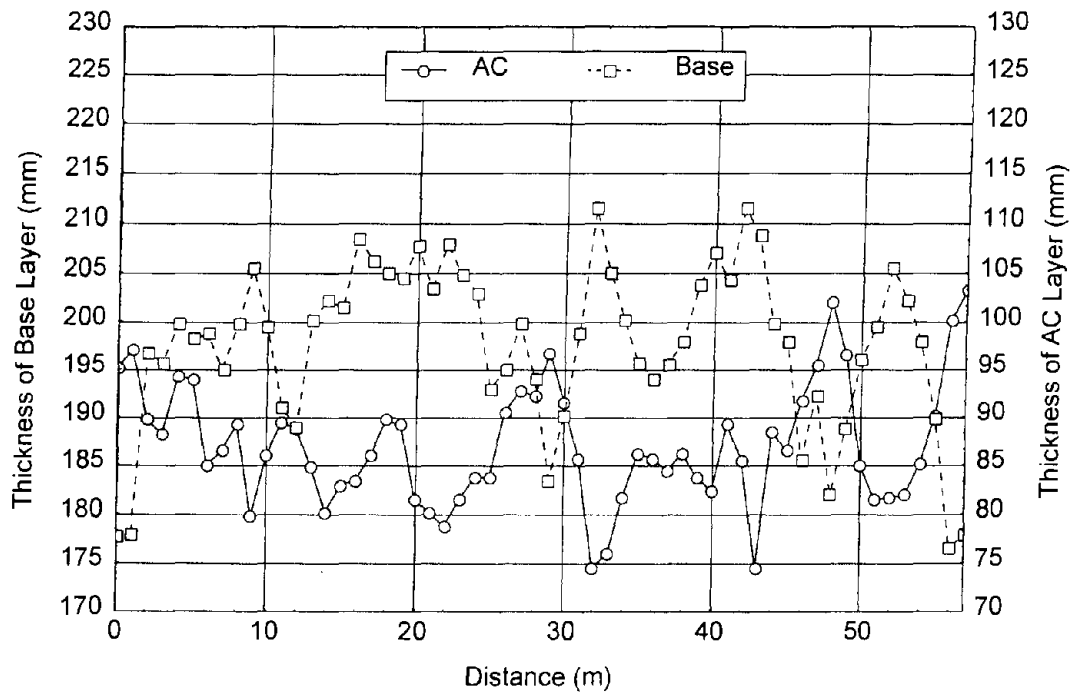


Figure 1. Layer Thickness, Inner Track

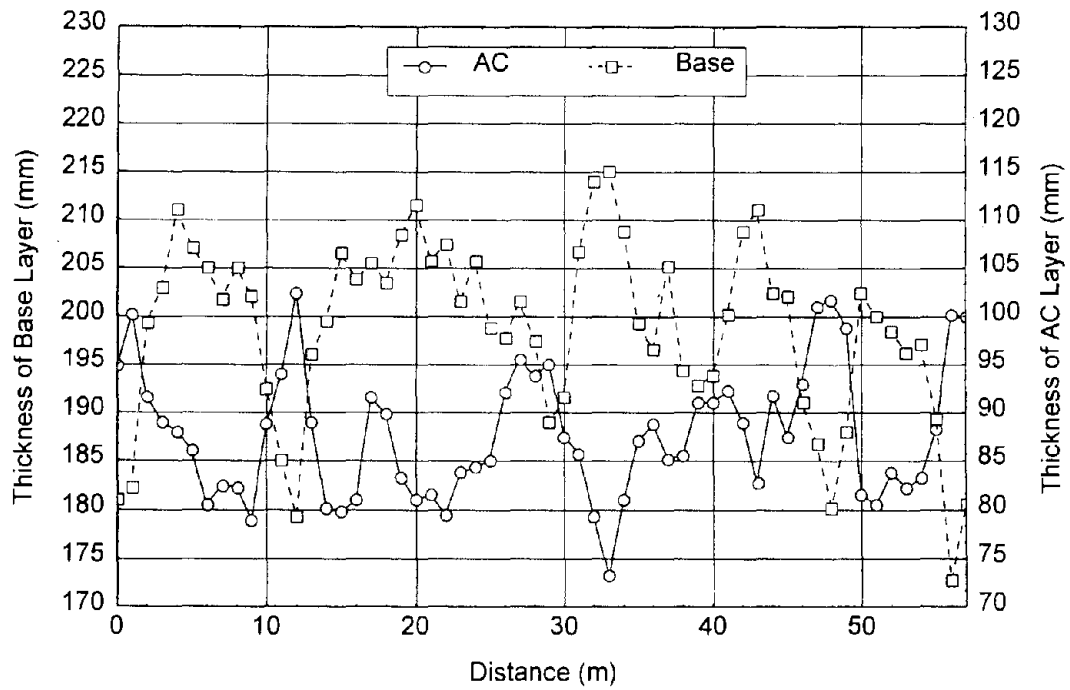


Figure 2. Layer Thickness, Outer Track

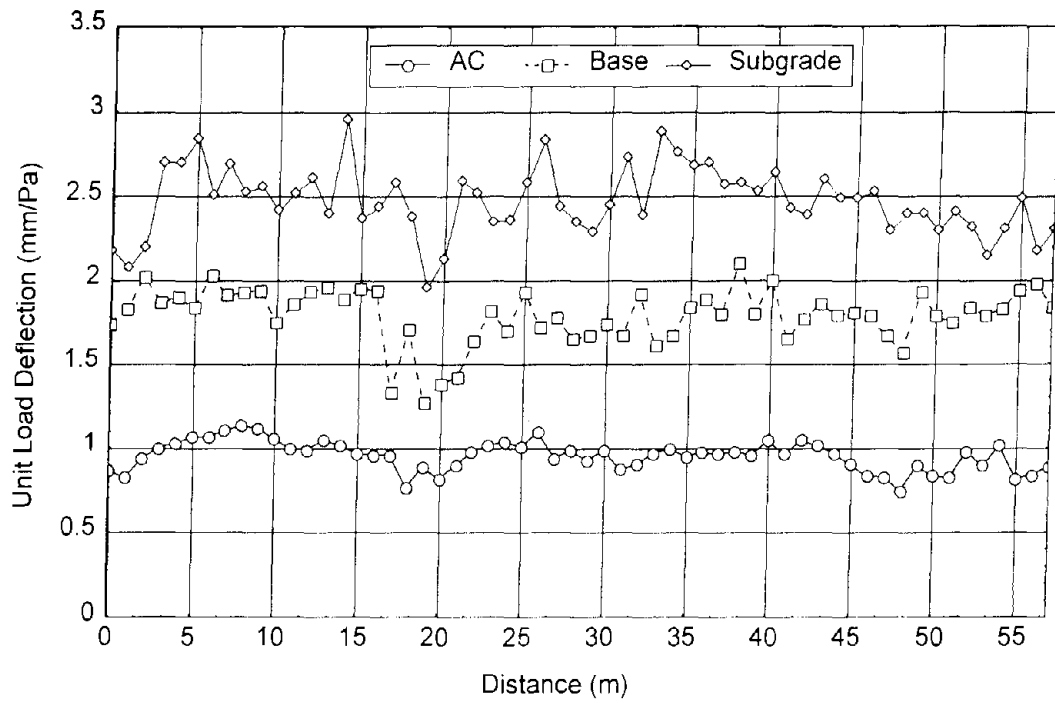


Figure 3. Unit Load Layer Deflection at Construction, Inner Track

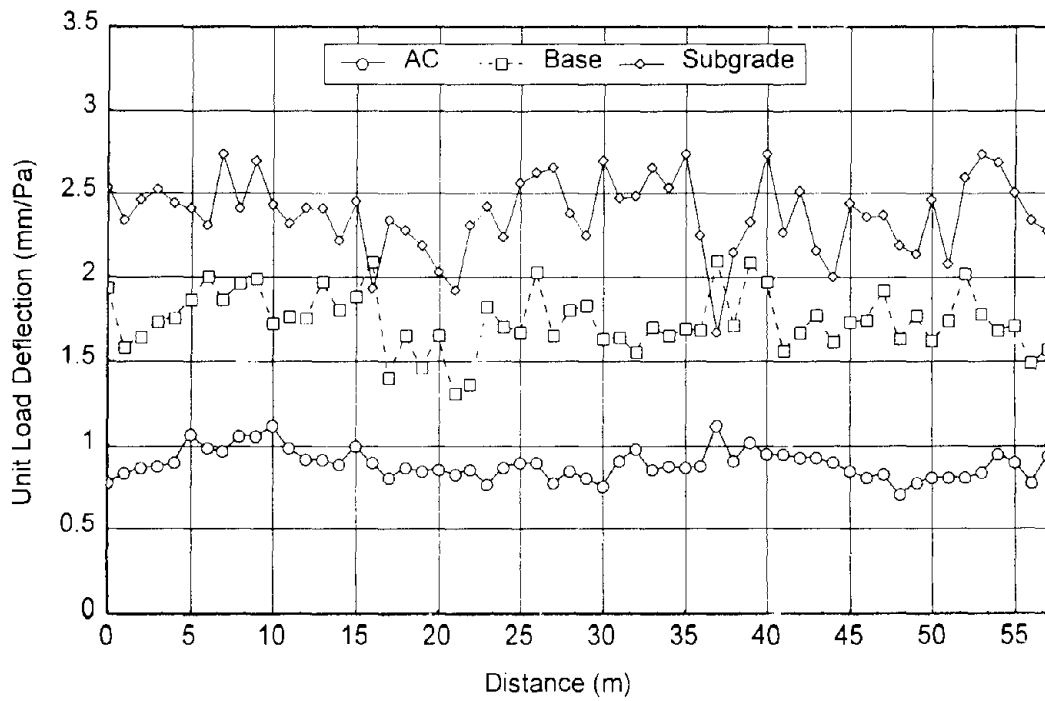


Figure 4. Unit Load Layer Deflection at Construction, Outer Track

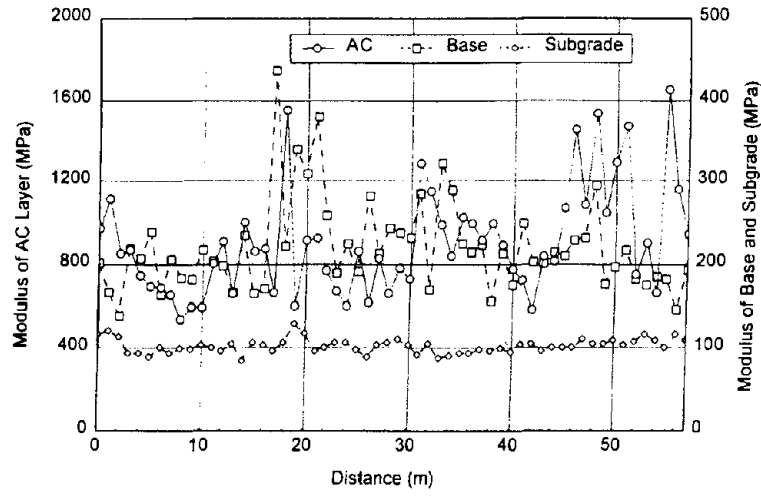


Figure 5. Layer Moduli, Inner Track (Initial)

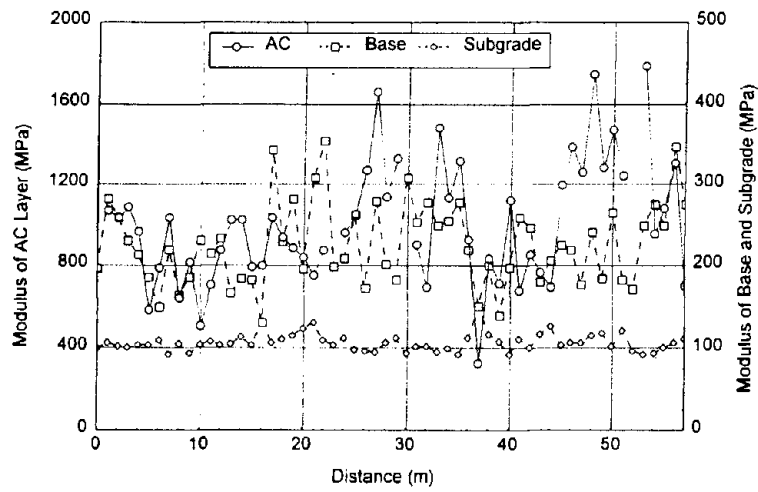


Figure 6. Layer Moduli, Outer Track (Initial)

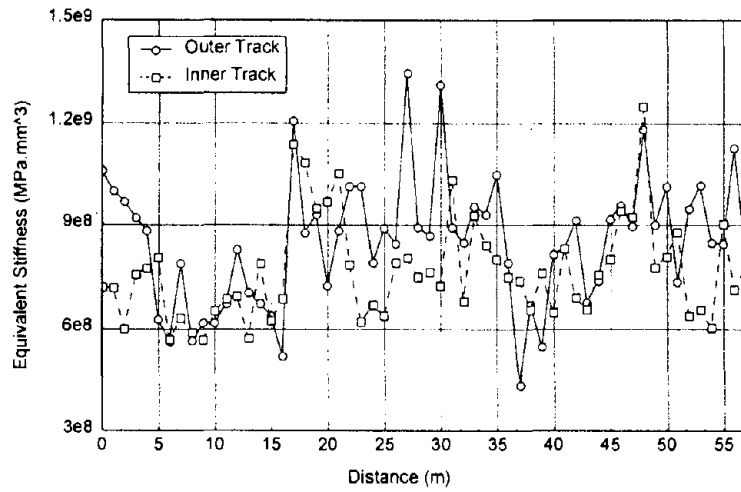


Figure 7. Equivalent Pavement Stiffness

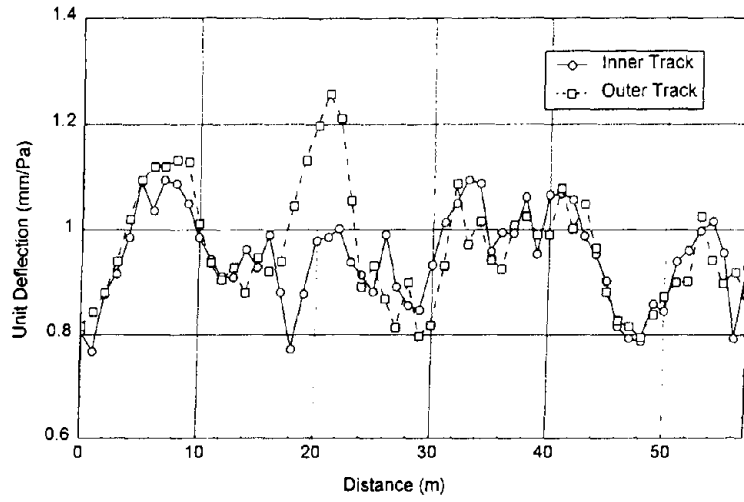


Figure 8a. Pavement FWD Surface Deflection at 20 k

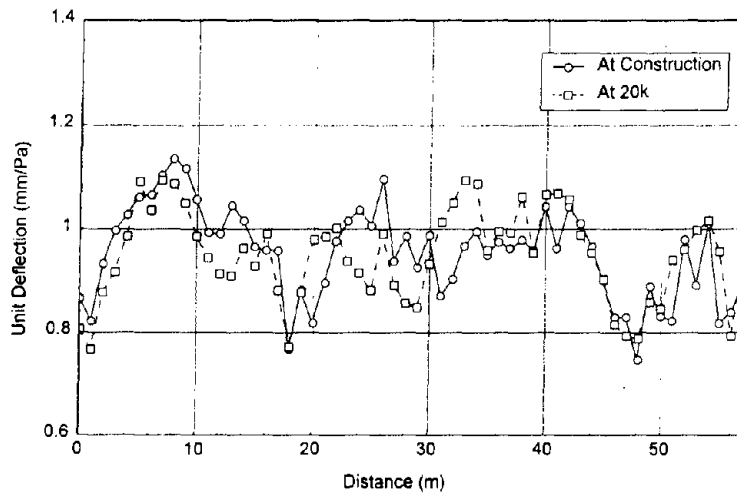


Figure 8b. Pavement FWD Surface Deflection, at Construction and at 20 k, Inner Track

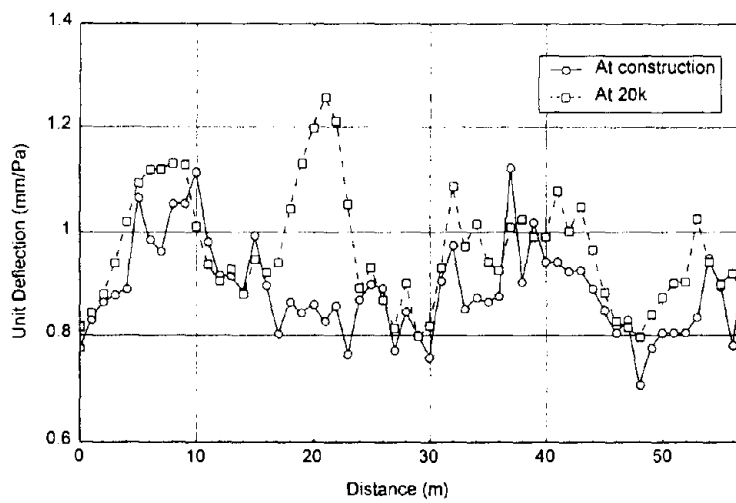


Figure 8c. Pavement FWD Surface Deflection, at Construction and at 20 k, Outer Track

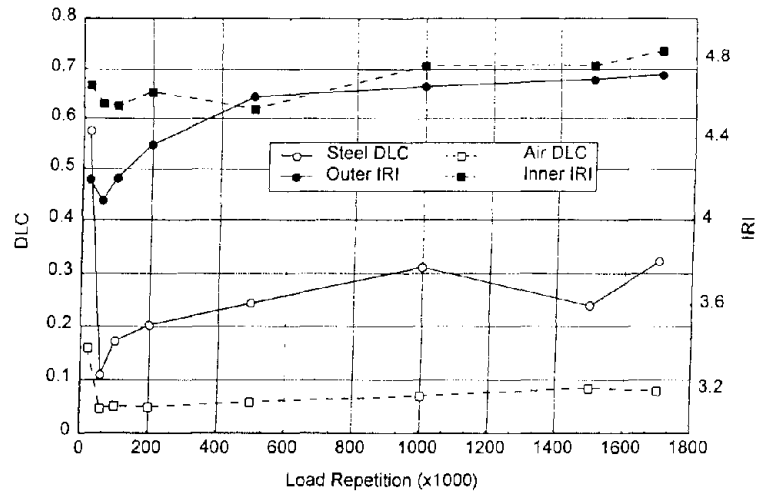


Figure 9. DLC and IRI vs. Load Repetitions

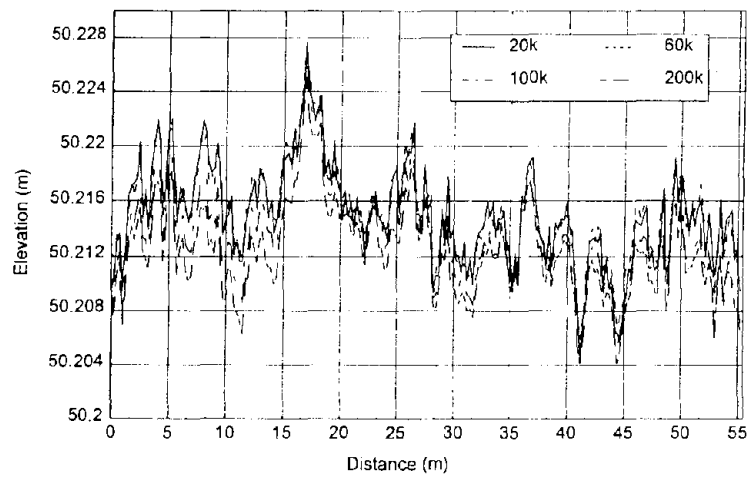


Figure 10a. Inner Track Profile at Different Load Repetitions

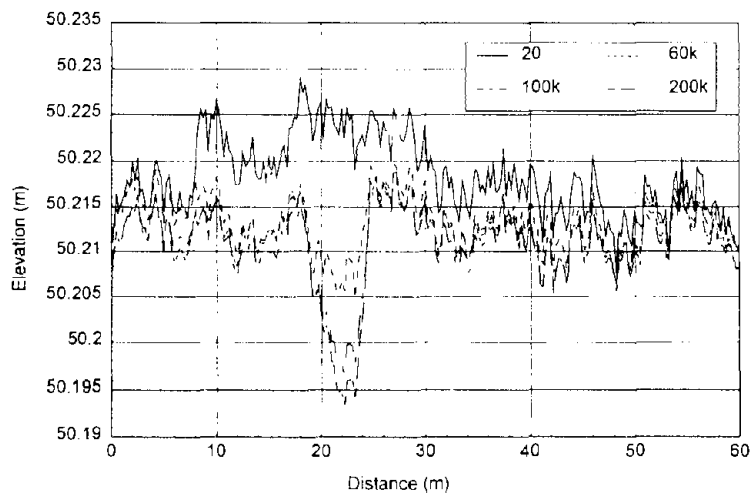


Figure 10b. Outer Track Profile at Different Load Repetitions

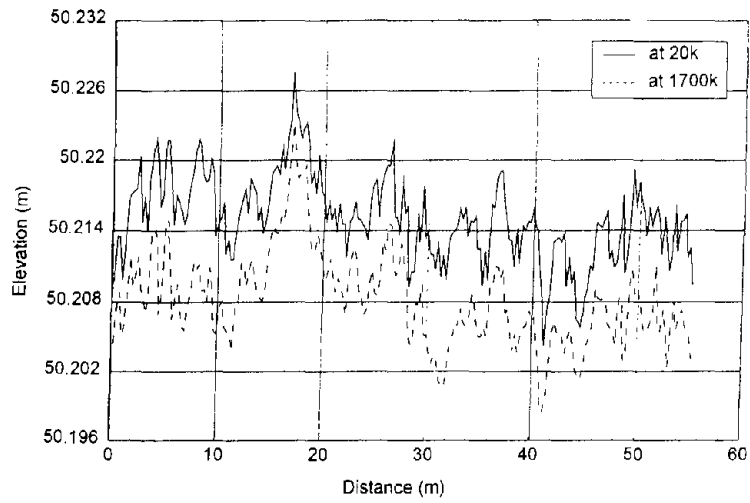


Figure 11a. Inner Track Profiles

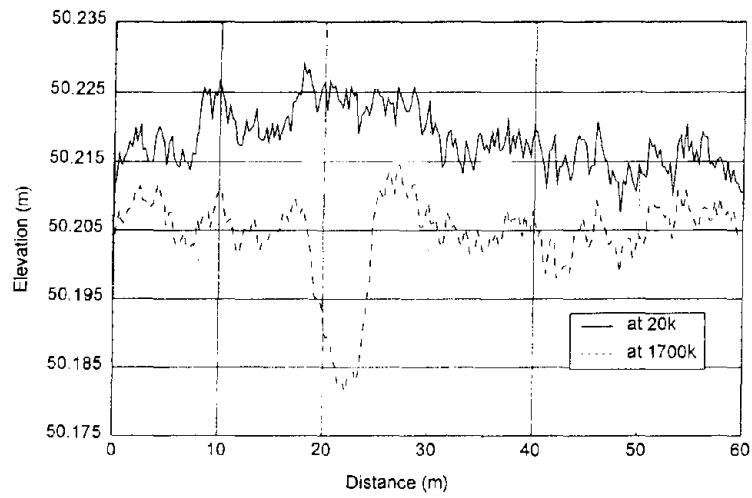


Figure 11b. Outer Track Profiles

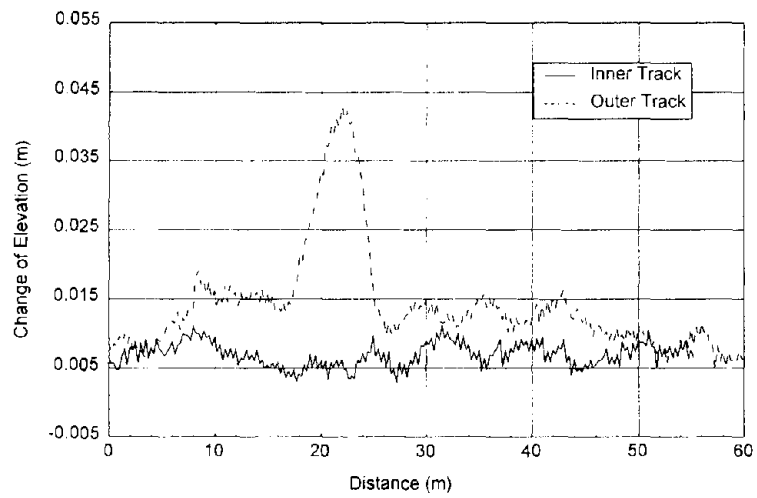


Figure 11c. Change of Profile from Beginning to End of Test

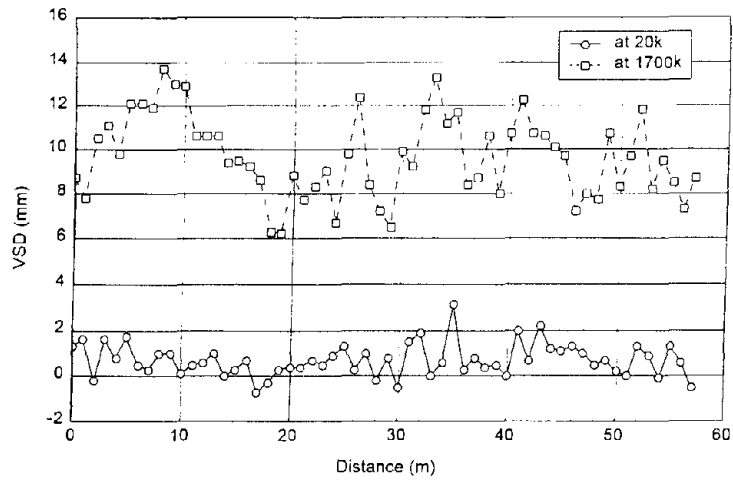


Figure 12a. Inner Track VSD

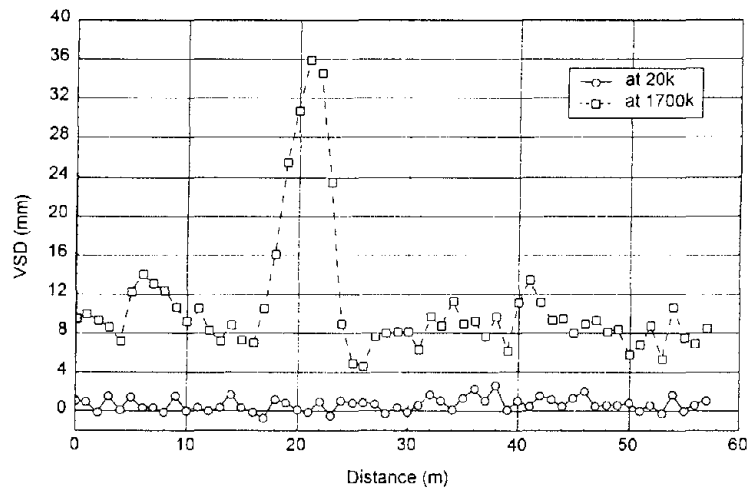


Figure 12b. Outer Track VSD

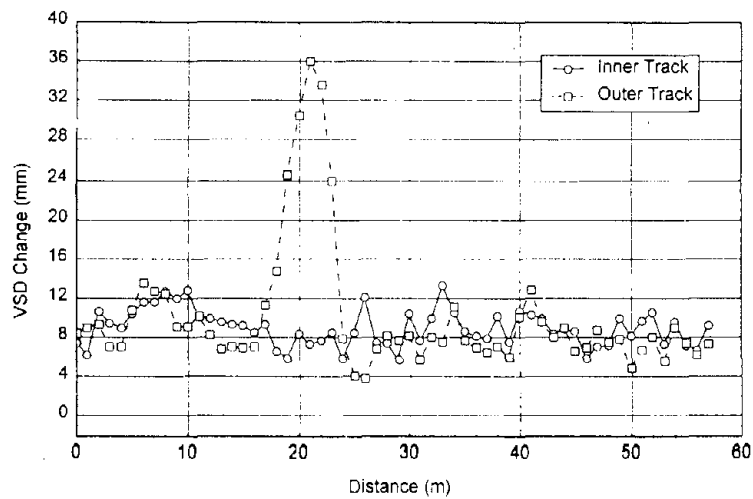


Figure 12c. Change of VSD from Beginning to End of Test

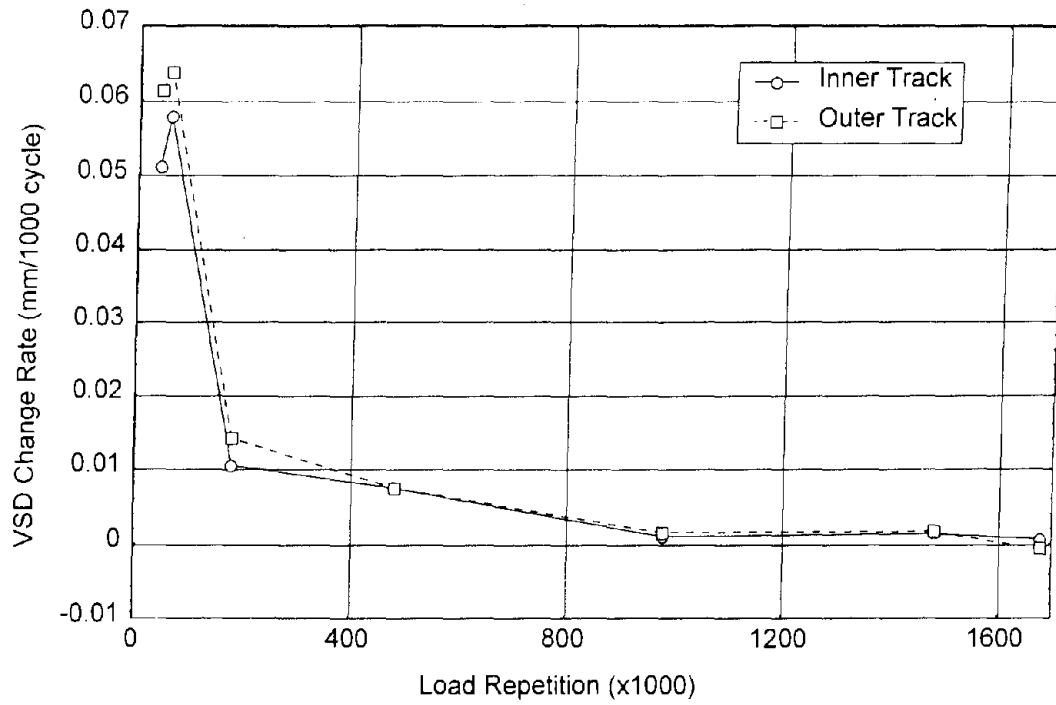


Figure 12d. Mean VSD Change Rate, All Data

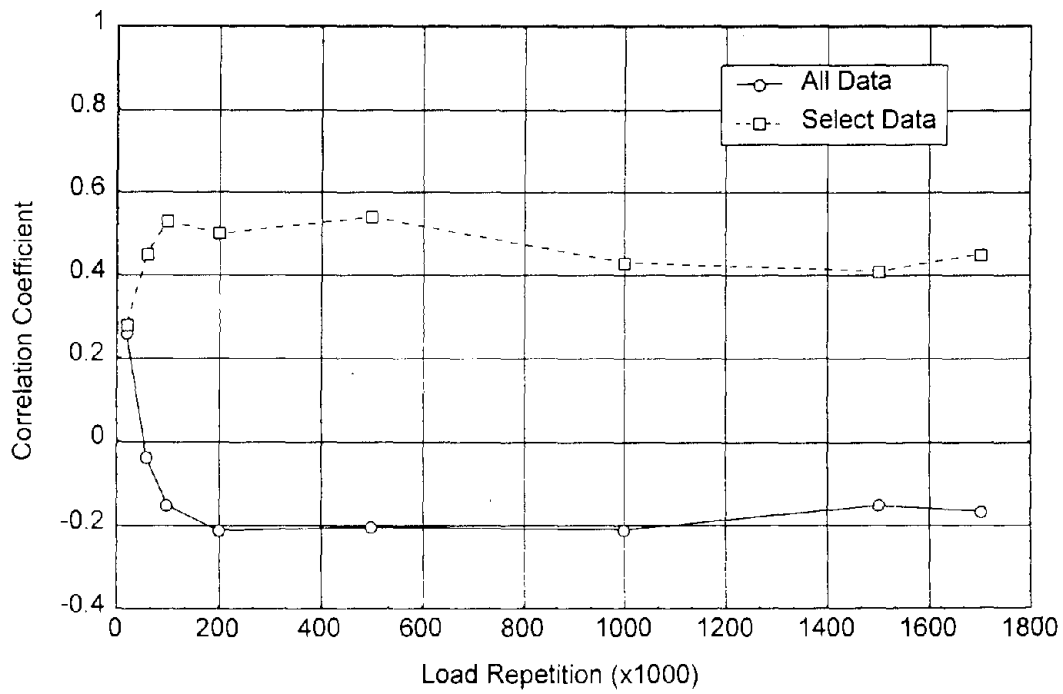


Figure 12e. Correlation Coefficient between Inner and Outer Track VSD

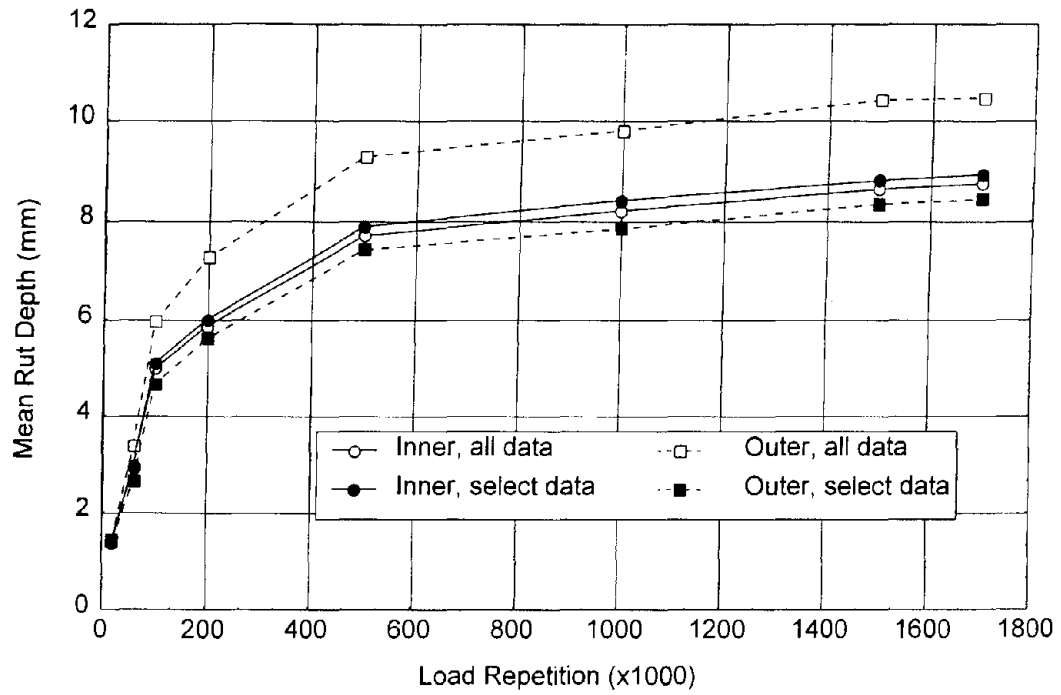


Figure 13a. Mean Rut Depth vs. Load Repetitions

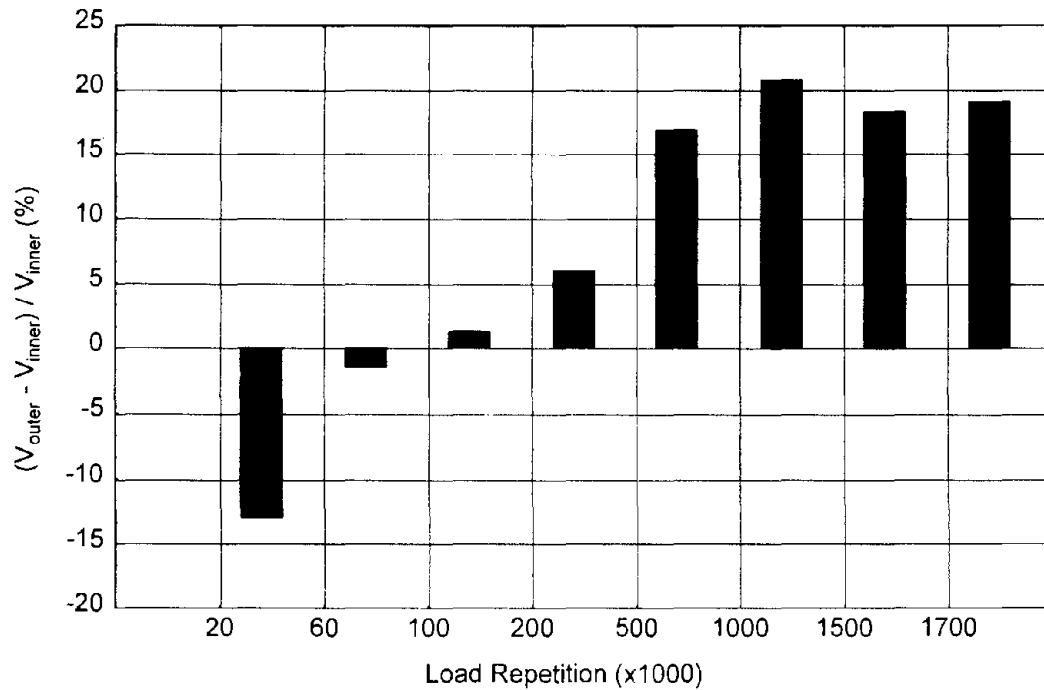


Figure 13b. Comparison of Rut Depth Variations of Outer and Inner Tracks, Select Data

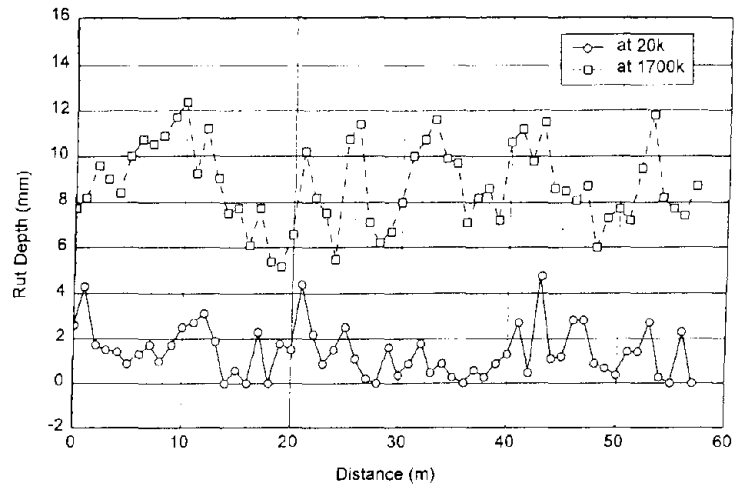


Figure 14a. Inner Track Rut Depth at Beginning and End of Test

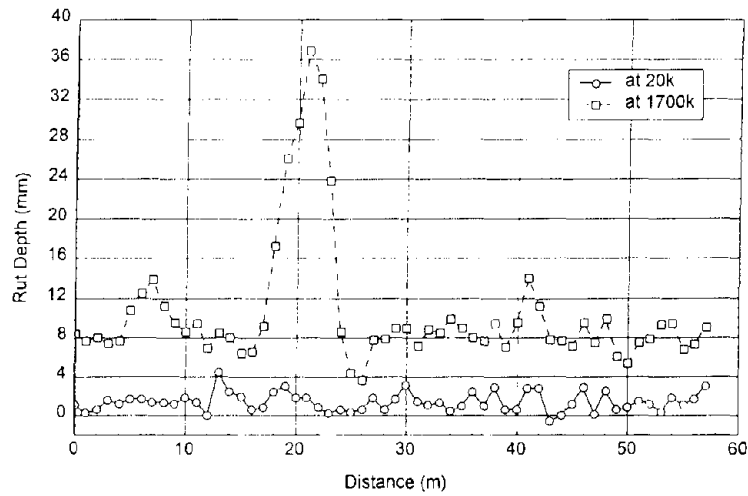


Figure 14b. Outer Track Rut Depth at Beginning and End of Test

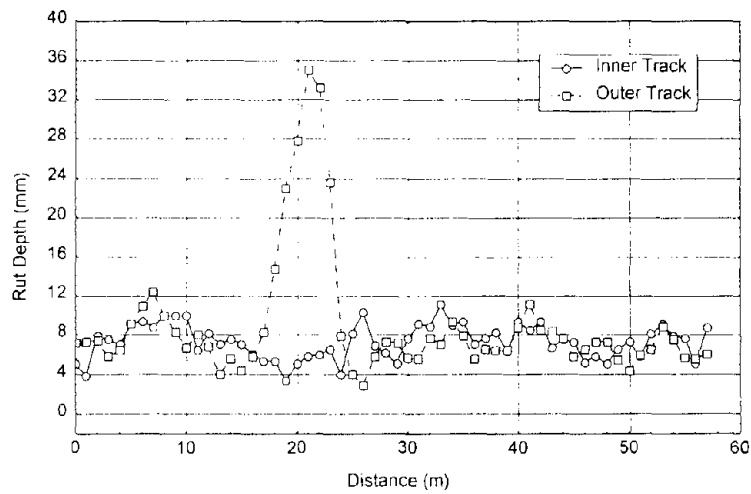


Figure 14c. Change of Rut Depth at Beginning and End of Test

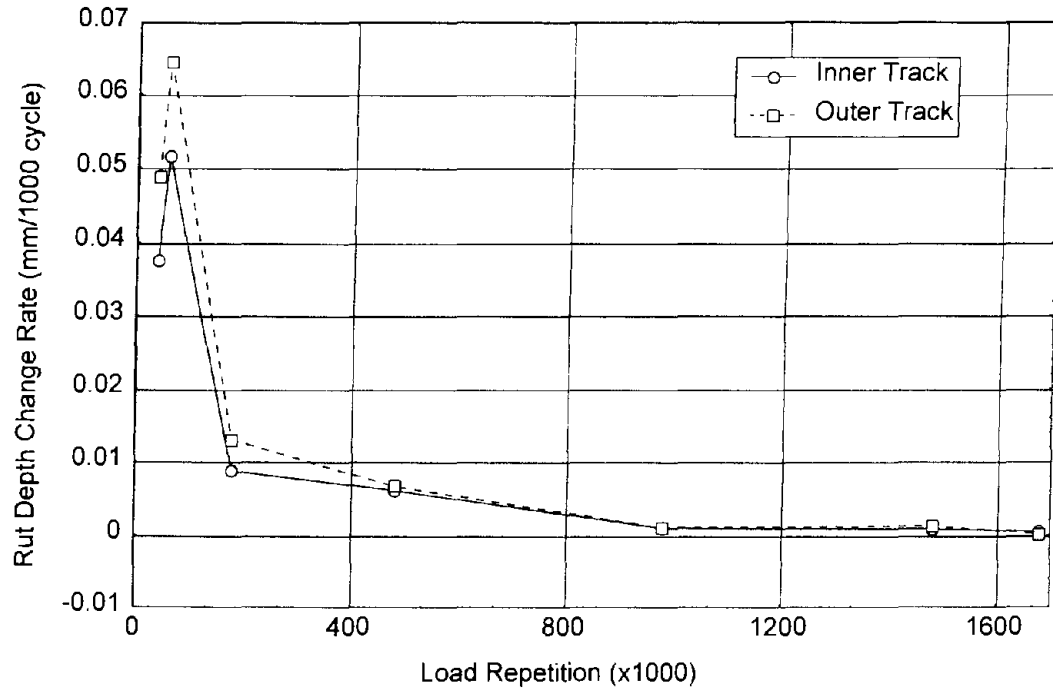


Figure 14d. Mean Surface Rut Depth Change Rate, All Data

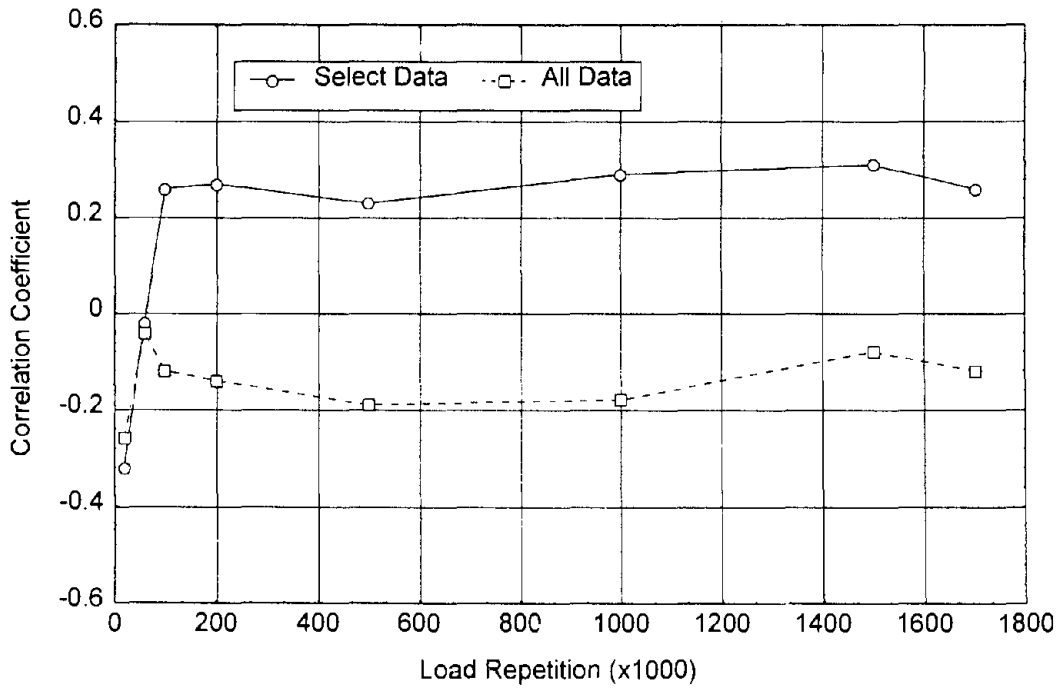


Figure 14e. Correlation Coefficient between Inner and Outer Track Rut Depth

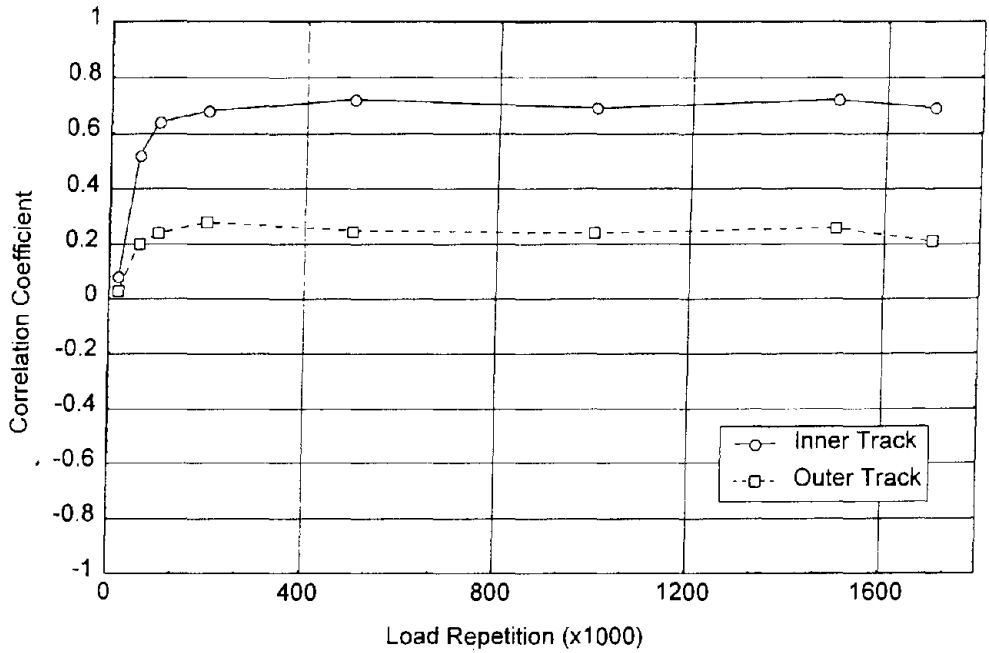


Figure 15. Cross Correlation between FWD Surface Deflection at 20 k and VSD (Inner - All Data, Outer - Select Data)

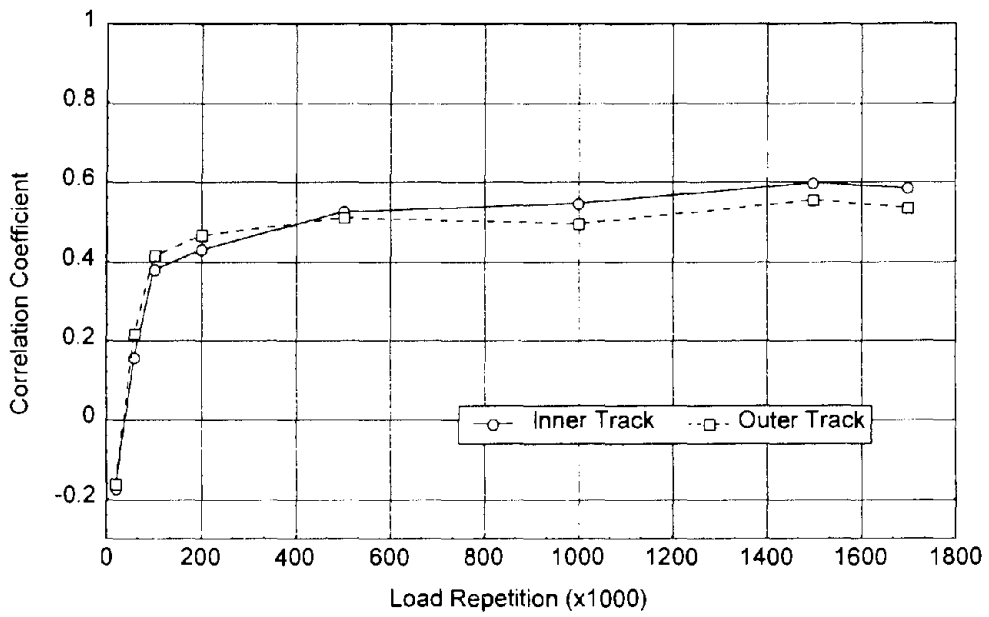


Figure 16. Cross Correlation between FWD Surface Deflection at 20 k and Rut Depth (Inner - All Data, Outer - Select Data)

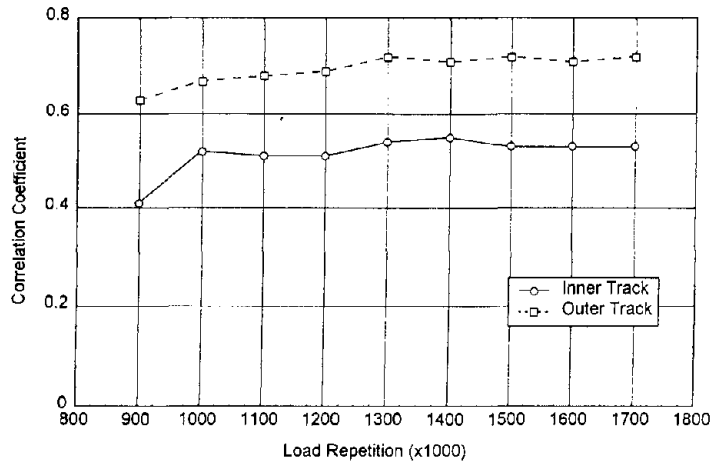


Figure 17a. Correlation between FWD Surface Deflection at 20 k and Total Linear Cracking (All Data)

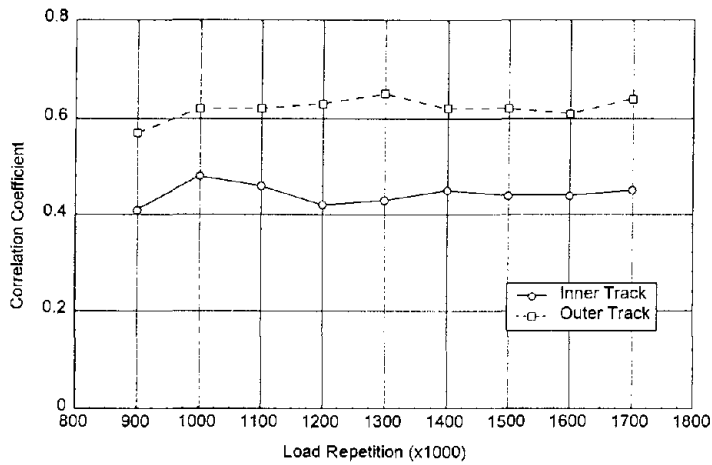


Figure 17b. Correlation between FWD Surface Deflection at 20 k and Longitudinal Linear Cracking (All Data)

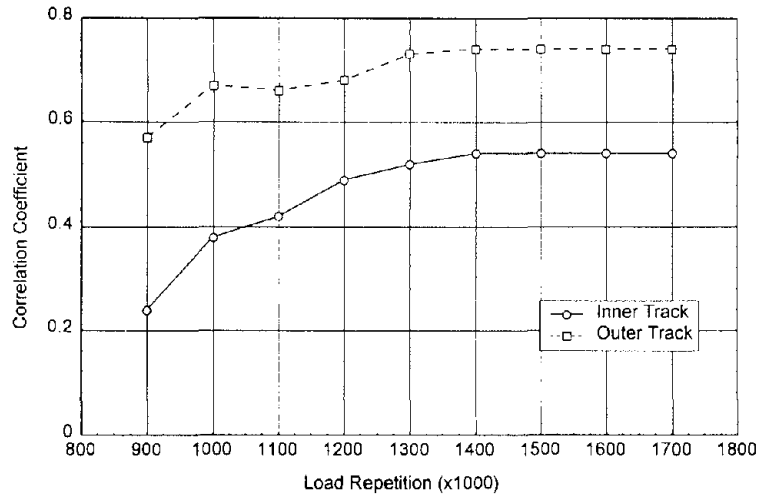


Figure 17c. Correlation between FWD Surface Deflection at 20 k and Transverse Linear Cracking (All Data)

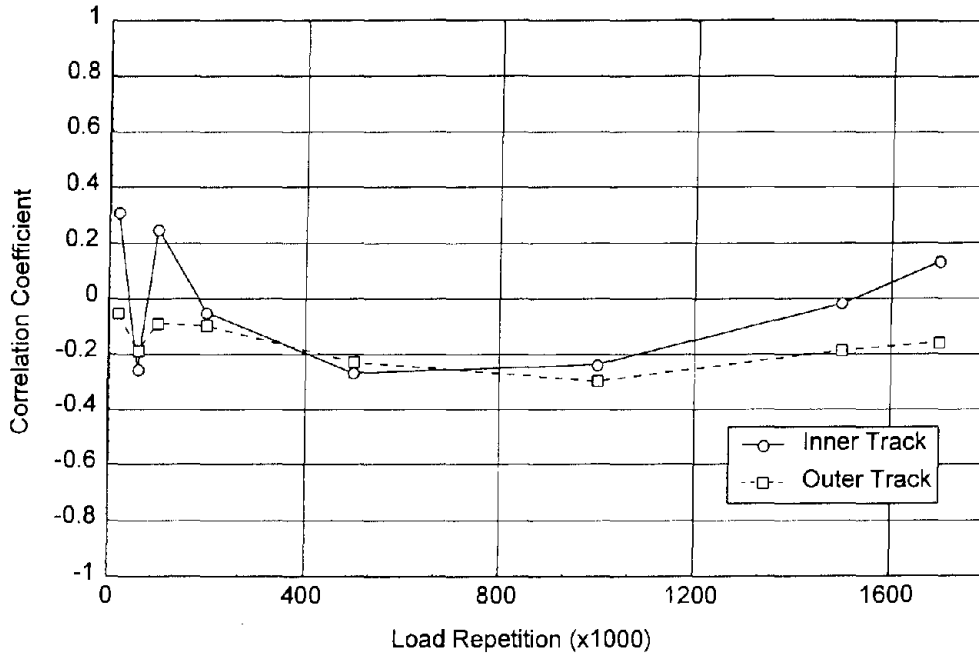


Figure 18. Cross Correlation between Wheel Force and FWD Surface Deflection at 20 k (Inner - All Data, Outer - Select Data)

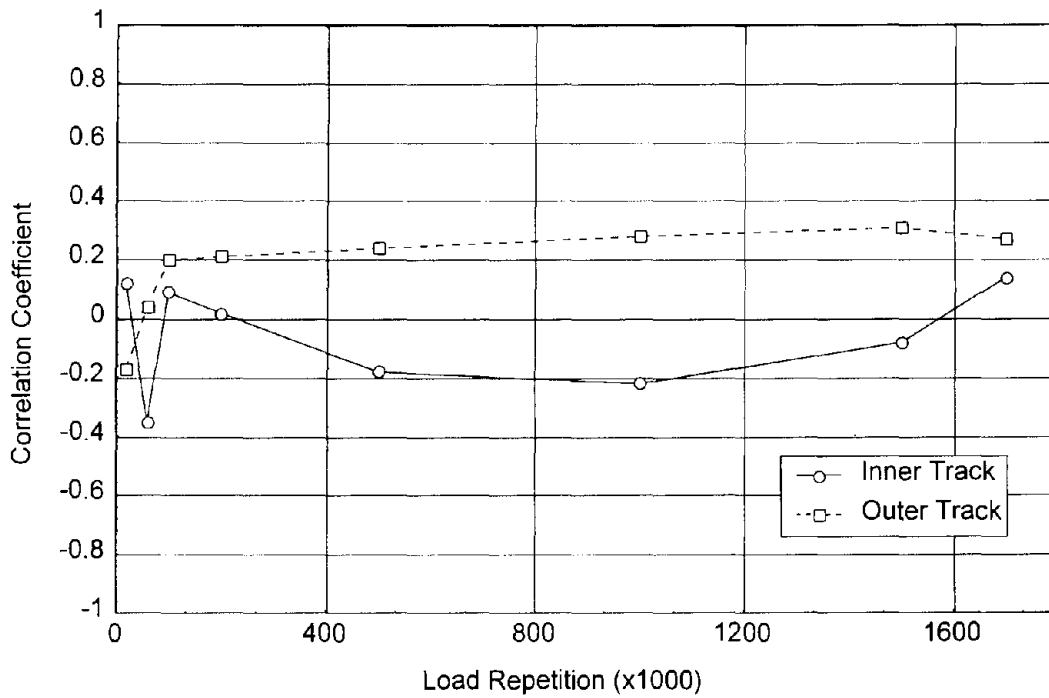


Figure 19. Cross Correlation between Wheel Force and VSD (Inner - All Data, Outer - Select Data)

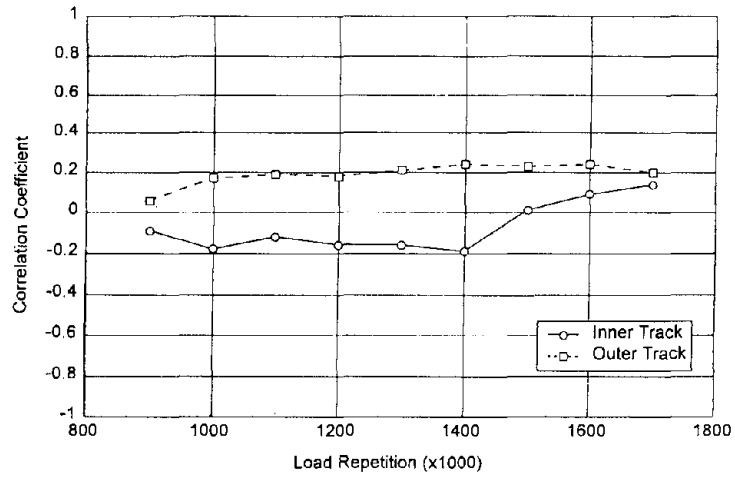


Figure 20a. Cross Correlation between Wheel Force and Total Cracking (All Data)

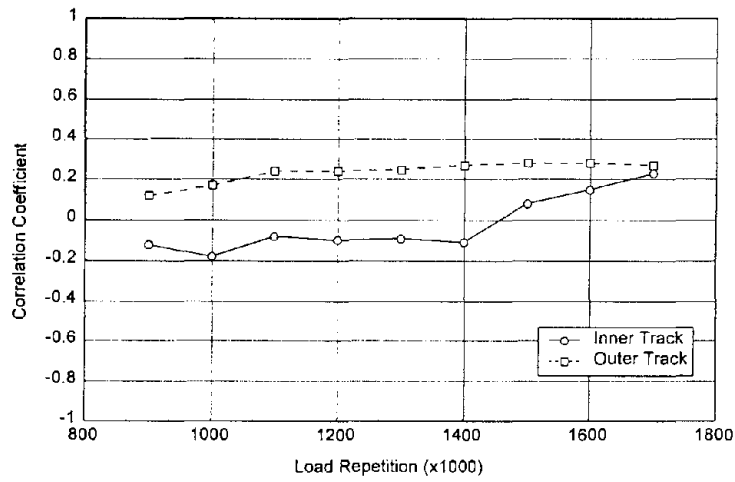


Figure 20b. Cross Correlation between Wheel Force and Longitudinal Cracking (All Data)

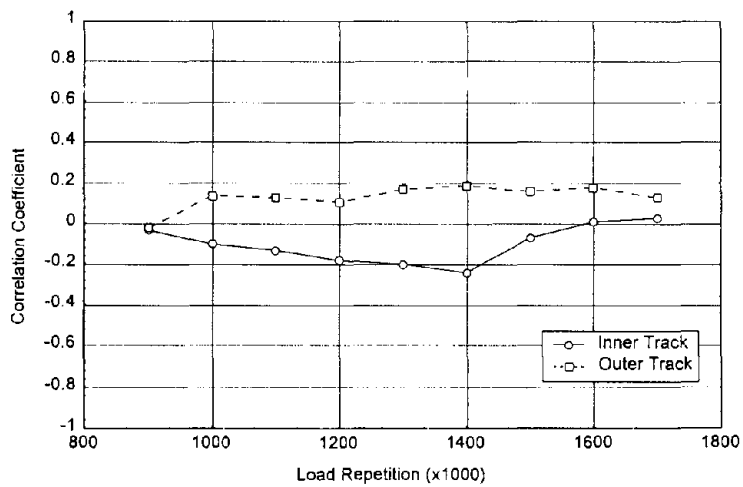


Figure 20c. Cross Correlation between Wheel Force and Transverse Cracking (All Data)

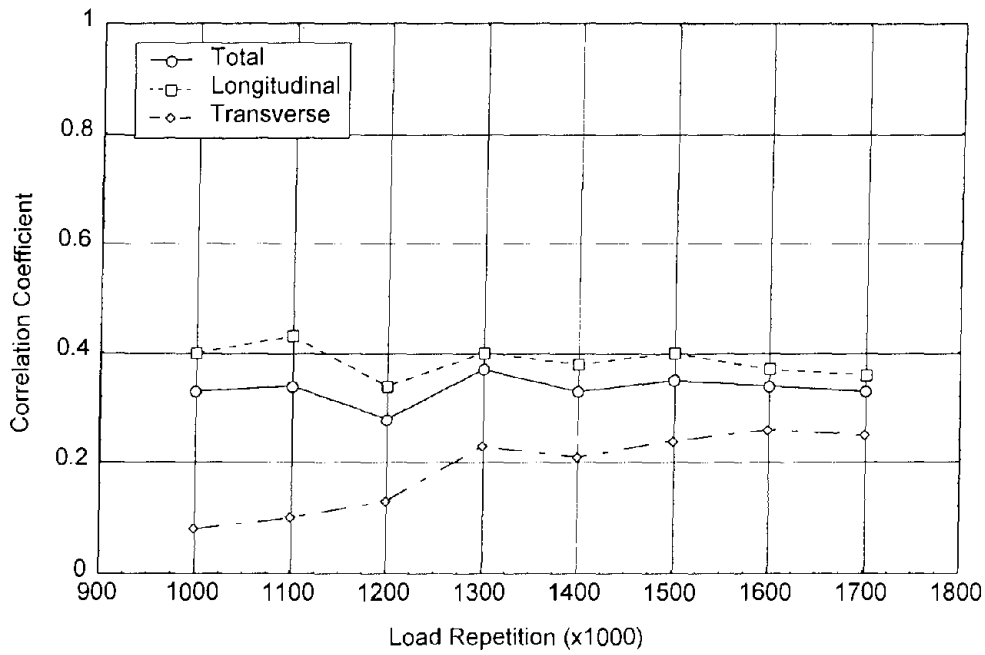


Figure 21a. Cross Correlation between Rut Depth and Linear Cracking Inner Track, All Data

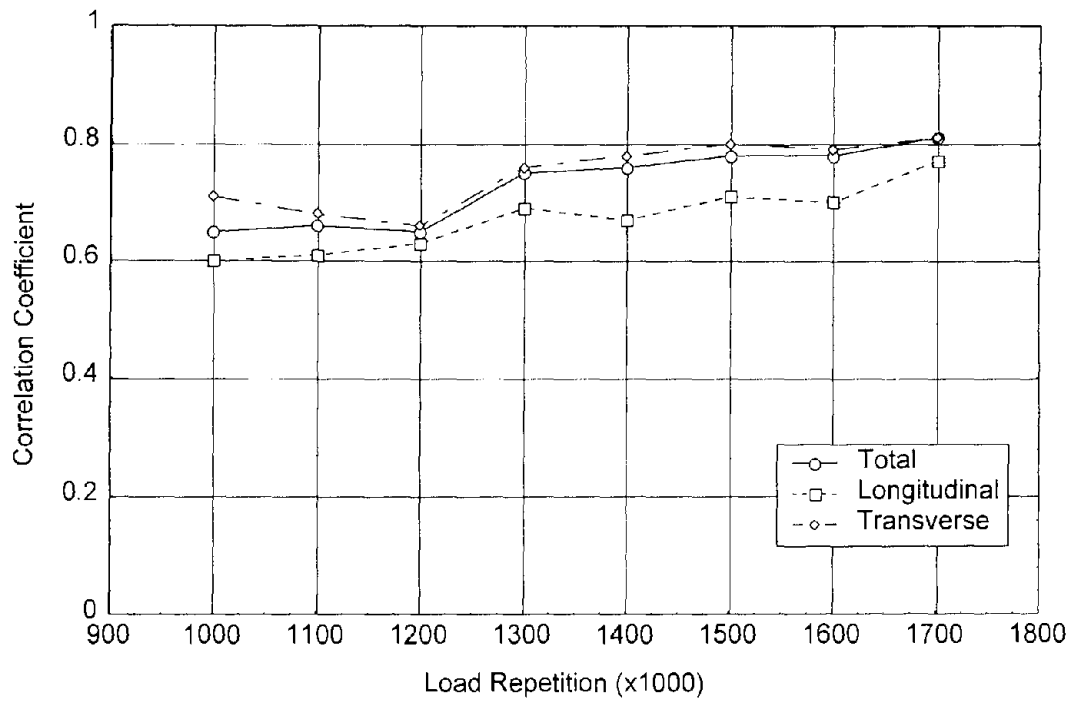


Figure 21b. Cross Correlation between Rut Depth and Linear Cracking Outer Track, All Data

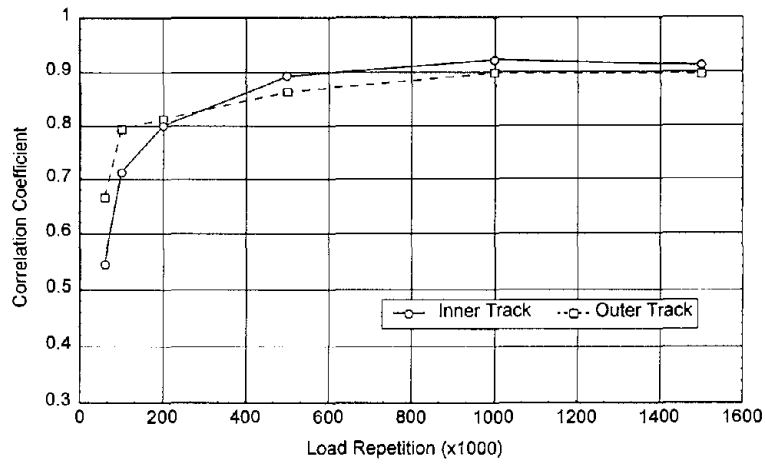


Figure 22. Correlation between Profile at 1700 k and Profiles at Other Load Repetitions (All Data)

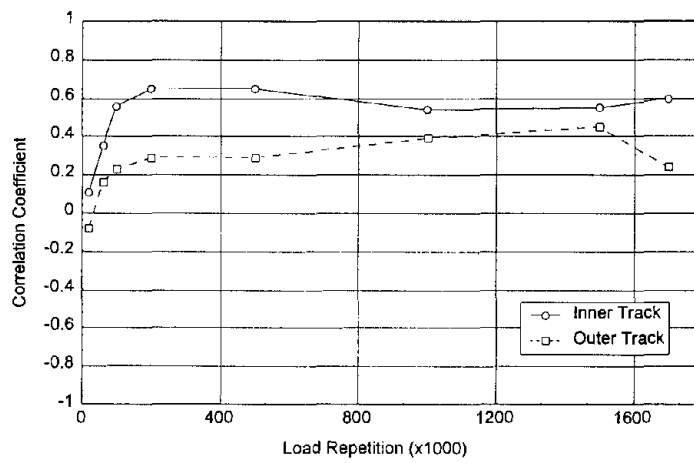


Figure 23. Cross Correlation between VSD and (Wheel Force*FWD) (Inner - All Data, Outer - Select Data)

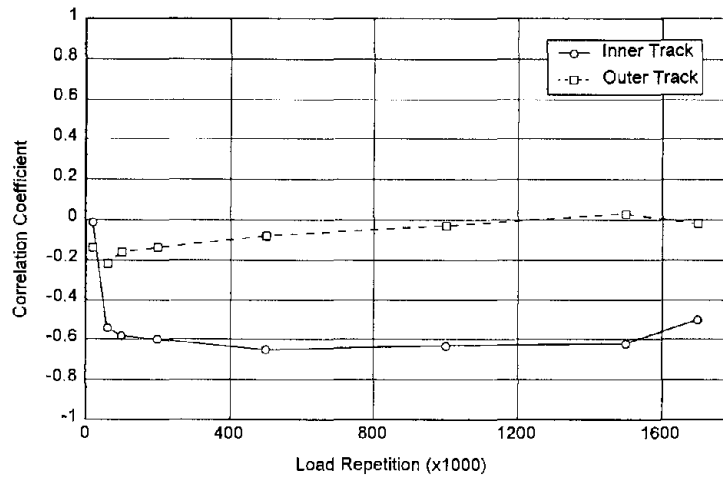


Figure 24. Cross Correlation between VSD and (Wheel Force/FWD) (Inner - All Data, Outer - Select Data)

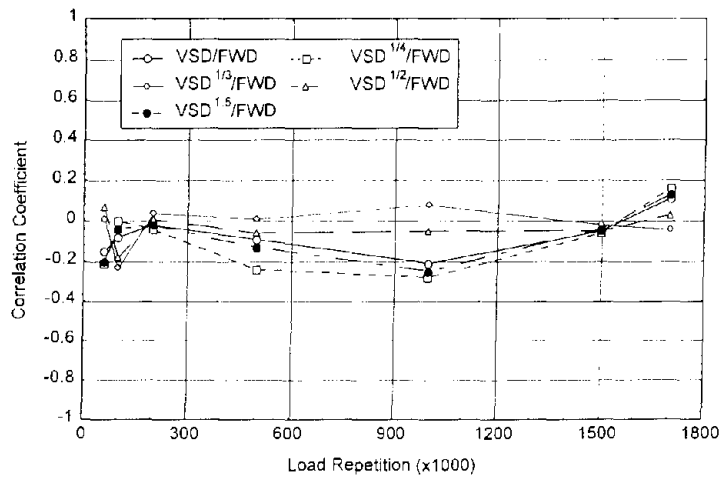


Figure 25a. Correlation between Wheel Force and (VSDⁿ/FWD), Inner Track (All Data)

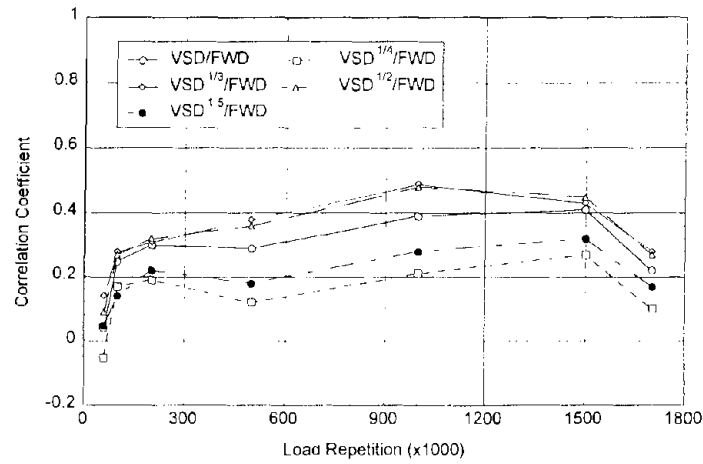


Figure 25b. Correlation between Wheel Force and (VSDⁿ/FWD), Outer Track (Select Data)

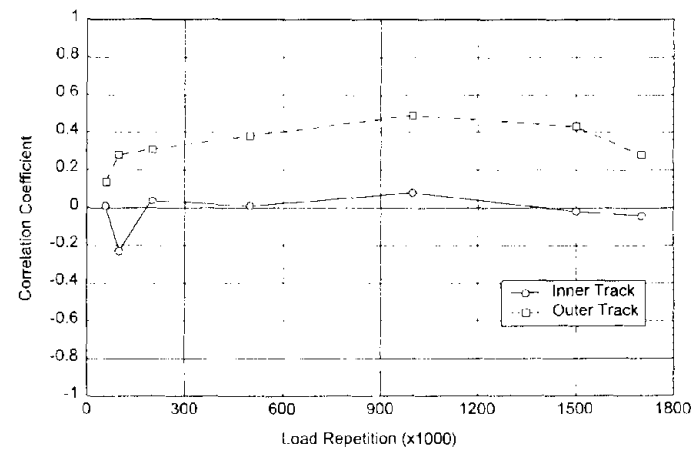


Figure 25c. Correlation between Wheel Force and (VSD^{1/3}/FWD) (Inner - All Data, Outer - Select Data)

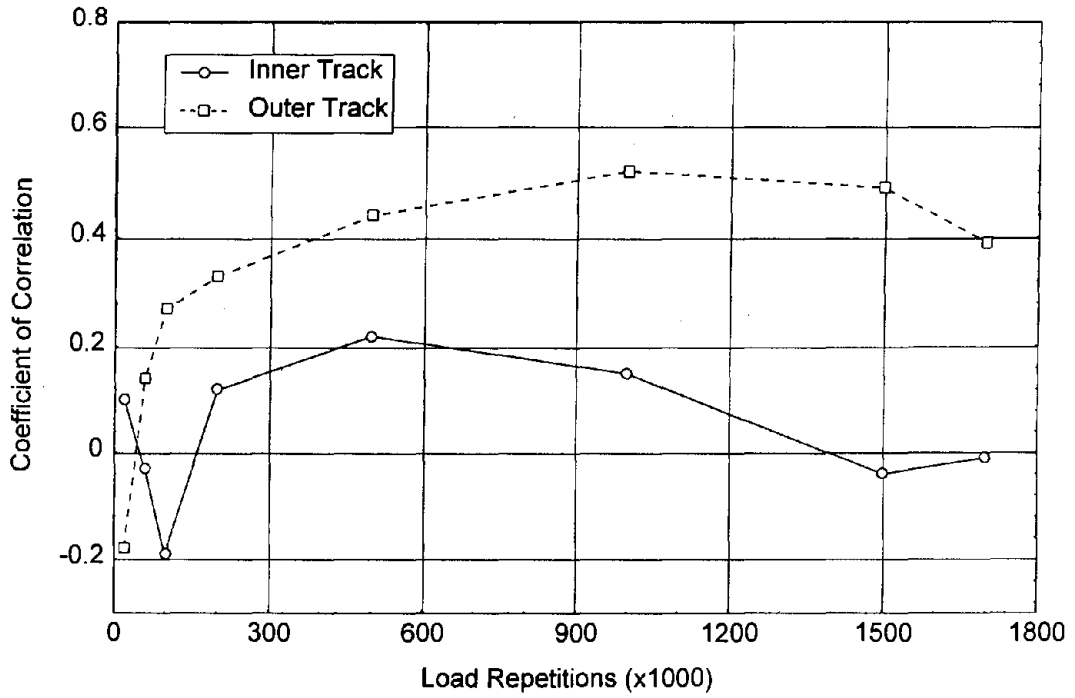


Figure 26a. Cross Correlation between Wheel Force and (VSD/FWD^3) , All Data

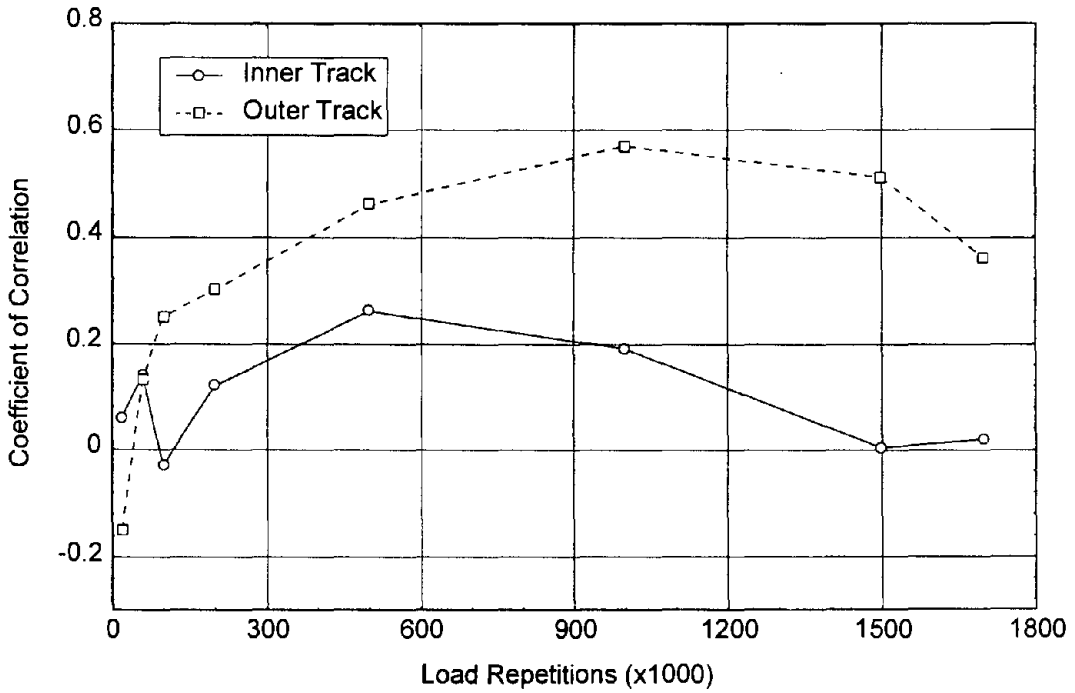


Figure 26b. Cross Correlation between Wheel Force and (VSD/FWD^3) , Select Data

REFERENCE

1. Fussell, A., B. Steven and B. Pidwerbesky, "DIVINE Element 1 Loading Report", Civil Engineering Research Report CERR96-5, University of Canterbury, Christchurch, New Zealand, May 1996.
2. AASHTO Guide for Design of Pavement Structures. Vol. 2. National Cooperative Highway Research Program, Transportation Research Board, National Research Council, NCHRP Project 20-7 (Task 24&28), August 1986.

